U.PORTO
FACULDADE DE CIÊNCIAS
UNIVERSIDADE DO PORTO

MSc

2.º CICLO

FCUP
2018

U.PORTO

Dissecting the Role of Caenorhabditis elegans Dynein Light Intermediate Chain in Neuronal Trafficking

Cátia Filipa Vieira de Carvalho

FC

Dissecting the Role of *Caenorhabditis elegans* Dynein Light Intermediate Chain in Neuronal Trafficking

Cátia Filipa Vieira de Carvalho

Dissertação de Mestrado apresentada à
Faculdade de Ciências da Universidade do Porto em
Biologia Celular e Molecular

2018

U.PORTO
FACULDADE DE CIÊNCIAS
UNIVERSIDADE DO PORTO

MSc

Dissecting the Role of *Caenorhabditis elegans* Dynein Light Intermediate Chain in Neuronal Trafficking

Cátia Filipa Vieira de Carvalho

Mestrado em Biologia Celular e Molecular

Departamento de Biologia

2018

Orientador

Reto Gassmann, Group Leader

Instituto de Investigação e Inovação em Saúde (i3S)

Coorientador

Ricardo dos Santos Celestino, Investigador Pós-Doutoramento

Instituto de Investigação e Inovação em Saúde (i3S)

Escola Superior de Saúde, Politécnico do Porto (ESS-IPP)

Todas as correções determinadas pelo júri, e só essas, foram efetuadas.
O Presidente do Júri,

Porto, _____/_____/_____

Autor

Cátia Filipa Vieira de Carvalho, FCUP, i3S

Rua do Campo Alegre, 4169-007 Porto, PORTUGAL, up201602951@fc.up.pt, 220 402 700

Orientador

Reto Gassmann, Group Leader, i3S

Rua Alfredo Allen, 4200-135 Porto, PORTUGAL, rgassmann@ibmc.up.pt, +351 220 408 800

Coorientador

Ricardo dos Santos Celestino, Investigador Pós-Doutorado, i3S, ESS-IPP

Rua Alfredo Allen, 4200-135 Porto, PORTUGAL, ricardo.celestino@ibmc.up.pt, +351 220 408 800

Eu, **Cátia Filipa Vieira de Carvalho**, aluna com o número 201602951 do Mestrado em Biologia Celular e Molecular da edição de 2016/2018, declaro sob compromisso de honra ser autora do texto apresentado, não sendo este plagiado. Declaro também que tomei conhecimento das consequências que advêm de situações de plágio.

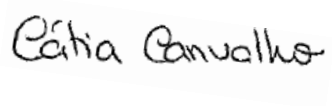

Porto, 28 de setembro de 2018

Cátia Filipa Vieira de Carvalho

ACKNOWLEDGMENTS

First of all, I would like to thanks to my supervisor, Reto. Thank you for your vision; I am grateful for your trust, teachings, and all the challenges. Your optimism and our talks always made my day better. Thank you!

Ricardo, mais do que co-orientador ou colega, terminamos este desafio como amigos. Obrigada pelas gargalhadas, pelos conselhos e por seres sempre sincero comigo. Foram anos de aprendizagem diária, possiveis apenas por teres acreditado em mim. Obrigada!

I read somewhere that when you are the smartest person in a room, you are on the wrong room. I confirm every day that I am on the right room. To all of the GCP lab members: you are the most inteligent people that I ever met; I learned more from you than I can tell. Thank you!

Importa ainda agradecer à Patrícia e à Joaninha por *always got my back*, pelo *no judgement* e pela *brutal honesty*; à Filipa, à Inês e à Adriana pelo exemplo de dedicação e pelas gargalhadas, na alegria e no desespero; à Cláudia, ao Bernardo, ao Daniel, à Tânia, ao Hélder e à Rita por serem exemplos de companheirismo, humildade e profissionalismo. Muito obrigada por todas as vezes em que não hesitaram em ajudar-me, aconselhar-me e ensinar-me.

Agradeço ao meus incríveis amigos, indecisos e decididos: Catarina, Francisca, Jéssica, Raquel, Sara, Simões, Pimenta e Salgado, Monteiro, Francisco. Obrigada pelas gargalhadas, pelos lanches improvisados, pela rota das tascas e pelo apoio nos momentos menos bons.

Agradeço à minha família, que tanto adoro e respeito. Aos meus queridos primos, às minhas primeiras e melhores amigas: Margarida, Catarina, Luísa, Rita. Somos todas irmãs de mães diferentes (e pais também, esperamos todas). Tenho um orgulho imenso em vocês: podem sempre contar comigo.

Ao Tiago Macedo que teima em não sair do meu lado. Cada gargalhada ao teu lado, é um folêgo de ar nesta vida. Todos os dias me fazes acreditar que “a vida é boa de se levar”. Obrigada pela paciência, firmeza e amor. Espero ter-te ao meu lado em cada decisão e desafio.

Finalmente, agradeço ao meu irmão, Tiago Miguel, e aos meus queridos pais, Manuel e Ana Maria. Vocês são as minhas raízes e o meu amor maior. Um “obrigada” nunca vai chegar.

do not choose the lesser life. do you hear me.
do you hear me.
choose the life that is. yours.
the life that is seducing your lungs.
that is dripping down your chin.

Nayyirah Waheed, nejma

ABBREVIATIONS

AAA+	ATPases associated with various activities
AD	Adulthood
ARID	Autosomal Recessive Intellectual Disability
ATP	Adenosine triphosphate
CFEOM	Congenital Fibrosis of the Extraocular Muscles
CGC	Caenorhabditis Genetic Center
CMT	Charcot-Marie-Tooth disease
CMT2B	Charcot-Marie-Tooth disease type 2
Cryo-EM	Cryo-electron microscopy
DHC	Dynein heavy chain
DIC	Dynein intermediate chain
DLC	Dynein light chain
DLIC	Dynein light intermediate chain
DTT	Dithiothreitol
ERC	Endosomal-recycling compartment
GFP	Green fluorescent protein
HR	Homologous repair
HSP	Hereditary Spastic Paraplegic
ID	Intellectual Disease
IFT	Intraflagellar transport
LB	Luria Broth
MAPs	Microtubule associated proteins
MCD	Malformations of Cortical Development
MDa	Megadalton
MHAC	Microhydronencephaly
MND	Motor Neuron Disease
MTBD	Microtubule binding domain
NGM	Nematode Growth Media
NHEJ	Non-homologous end-joining
PAM	Protospacer adjacente motif
PCR	Polimerase chain reaction
PNK	T4 Polynucleotide kinase
RFLP	Restriction-fragment length polymorphism
RNA	Ribonuclei acid
RNP	Ribonucleoproteins
SDS-PAGE	Sodium dodecyl sulfate polyacrylamide gel electrophoresis
SEM	Standard error of the mean
sgRNA	single-guide RNA
SMA-LED	Lower Extremity Dominant
SOC	Super optimal broth
TCTEX	T-Complex Testis-specific protein 1
TIRF	Total internal reflection fluorescence

RESUMO

O transporte axonal é essencial para a função neuronal, estando várias doenças neurodegenerativas e de desenvolvimento neuronal associadas a mutações nos mecanismos de transporte neuronal. A dineína 1 citoplasmática (dineína) é uma proteína motora, responsável pelo transporte retrógrado de cargas ao longo dos microtúbulos, transportando proteínas, mRNA e organelos dos terminais axonais para o corpo celular dos neurónios. Contudo, os mecanismos de recrutamento e ativação das funções da dineína são pouco conhecidos. Vários estudos mostram que vários adaptadores da dineína, que tranportam cargas específicas, ligam-se a uma hélice conservada na região desordenada da região C-terminal (hélice1) de uma das subunidades da dineína, a cadeia leve intermediária da dineína (DLIC).

Para estudar a função da hélice1 *in vivo,* introduzimos mutações no gene ortólogo DLIC do animal *C. elegans* - *dli-1*, que dissociam a ligação da DLI-1 aos adaptadores, editando o genoma através da técnica CRISPR-Cas9. As mutações pontuais na DLI-1^{helice1} causam esterilidade, encurtam o tempo de vida e dificultam a locomoção dos animais; um fenótipo consistente com fenótipos já descritos associados a mutantes na dineína. Investigamos ainda a distribuição de endossomas e vesículas sinápticas em neurónios nos animais mutantes, confirmando que a mobilidade de cargas é afetada severamente, à semelhança do que é reportado na literatura relativamente a animais com depleções de dineína. Além disso, investigamos a distribuição das mitocôndrias ao longo dos neurónios e não encontramos alterações nos animais mutantes, no entanto observamos um aumento na densidade mitocondrial ao longo dos neurónios. Estes resultados mostram que a mutação da DLIC^{DLI-1} helix1 em *C. elegans* interfere no transporte de cargas mediado pela dineína nos neurónios.

A perturbação das funções de transporte da dineína parecem potenciar o processo de neurodegeneração observado por encurtar a vida dos animals e comprometer a sua locomoção, confirmando a importância da interação entre a DLIC com as proteínas adaptadoras, *in vivo*.

PALAVRAS-CHAVE

dineína citoplasmática 1; transport retrógrado axonal; cadeia leve intermediária da dineína; *Caenorhabditis elegans*; cargas

ABSTRACT

Axonal transport is essential for neuronal function, and several neurodegenerative and neurodevelopmental diseases are associated with mutations in neuron transport machinery. Cytoplasmic dynein 1 (dynein) is responsible for mostly all retrograde transport (minus-end directed) in axons; transporting proteins, mRNA, and organelles from the axon terminal towards the cell body. The regulation and activation of dynein functions remains poorly understood. Many cargo-specific adaptors for dynein have been shown to bind a conserved helix (helix1) in the disordered C-terminal region of dynein light intermediate chain (DLIC).

To study the function of the helix1 *in vivo,* we used CRISPR-Cas9 mediated genome editing to introduce mutations into the *C. elegans* DLIC othologue, *dli-1*, that disrupt the binding of DLI-1 with adaptors. Point mutations in the DLI-1 helix1 cause sterility, shorten lifespan, and impair locomotion, consistent with previous phenotypes associated with dynein mutants. We also directly examined the distribution of early endosomes and synaptic vesicles in neurons, and found them to be severely perturbed in helix1 mutants, identical to what is observed when the entire DLI-1 C-terminal region is deleted. Additionally, we have studied the distribution of mitocondria along the axon and found it to be not altered. However, we saw an increase in the mithocondrial density. These results show that mutating the $DLIC^{DLI\text{-}1}$ helix1 in C. elegans dirupt the dynein-mediated cargo transport in neurons.

The disruption of dynein transport functions appear to enhance the process of neurodegeneration observed by shorten lifespan, and impairment in locomotion, confirming that the interaction between DLIC with the adaptor proteins is also important *in vivo.*

KEYWORDS

Cytoplasmic dynein 1; axonal retrograde transport; dynein light intermediate chain; *Caenorhabditis elegans*; cargos

INDEX

LIST OF TABLES

LIST OF FIGURES

I. STATE OF ART

1. NEURONAL TRANSPORT AND TRAFFICKING

Neurons are highly differentiated cells, which have extensive processes that can achieve several meters in length in some species. The communication between those processes and the cell body is essential for the neuronal function and survival (Chevalier-larsen and Holzbaur, 2006; Maday et al., 2014). Axons link the cell body to the neuron terminals, and axonal transport of several organelles, such as signaling vesicles, is crucial for neuronal function. Mutations in proteins involved in the neuronal transport machinery (e. g. motor proteins, cytoskeleton structures, and cargo-associated proteins) lead to the disruption of the axonal transport being associated with several neurodegenerative and neurodevelopmental diseases (Table 1).

Table 1 – Neurodegenerative and neurodevelopmental diseases associated with mutations in axonal transport machinery. Adapted from Maday et al., 2014.

PROTEIN	GENE(S) WITH KNOWN MUTATION(S)	DISEASE(S)
Dynein	DYNC1H1	CMT, SMA-LED, ID, MCD (Epilepsy)
Dynactin	DCTN1	Perry syndrome, MND
BICD2	BICD2	SMA, HSP
Lis-1	PAFAH1B1	Lissencephaly
NDE1	NDE1	Microcephaly, MHAC
Rab7	RAB7A	CMT2B
CLIP-170	CLIP1	ARID
Microtubules	TUBA1A, TUBA8, TUBG1, TUBB3, TUBB2B	Lissencephaly, MCD, microcephaly, polymicrogyria, CFEOM

CMT – Charcot-Marie-Tooth disease; SMA-LED/SMA – Spinal Muscular Atrophy; ID – Intellectual Disease; MCD – Malformations of Cortical Development; MND – Motor Neuron Disease; HSP – Hereditary Spastic Paraplegic; MHAC - Microhydronencephaly; CMT2B - Charcot-Marie-Tooth disease type 2; ARID – Autosomal Recessive Intellectual Disability; CFEOM – Congenital Fibrosis of the Extraocular Muscles

Axonal transport occurs along the neuronal cytoskeleton that is composed by three major components: microtubules, actin filaments, and intermediate filaments (Chevalier-larsen and Holzbaur, 2006; Maday et al., 2014). The neuronal cytoskeleton provides structural support and it allows the cell to grow or change its size/shape.

Microtubules are polarized polymers of αβ-tubulin dimers with fast growing plus-ends and more stable minus-ends being indispensable for neuronal trafficking. In neurons, dendrites and axons have different microtubule orientations. Along the axon, the microtubules form a parallel arrangement with the plus-ends oriented towards axon terminals and the minus ends oriented towards the cell body [Figure 1 (Stepanova et al., 2003; Rao and Baas, 2017)]. The stabilization of the microtubule arrangement is possible due to microtubule-associated proteins (MAPs) that are present in higher concentrations in neurons compared to other cell types (Dixit et al., 2008), and due to the enrichment of post-translational modifications such as acetylation, detyrosination, phosphorylation, and polyglutamylation in axonal microtubules (Nirschl et al., 2017).

Two types of axonal transport take place on microtubules: anterograde (plus-end directed), and retrograde (minus-end directed) (Maday et al., 2014). The anterograde transport, towards the axon terminals, is responsible for the supply of newly synthesized proteins in the cell body to the different regions of the neurons. On the other hand, the cell body is the primary site for degradation of misfolded or aggregated proteins that need to be transported from the axon terminal towards the cell body by retrograde transport.

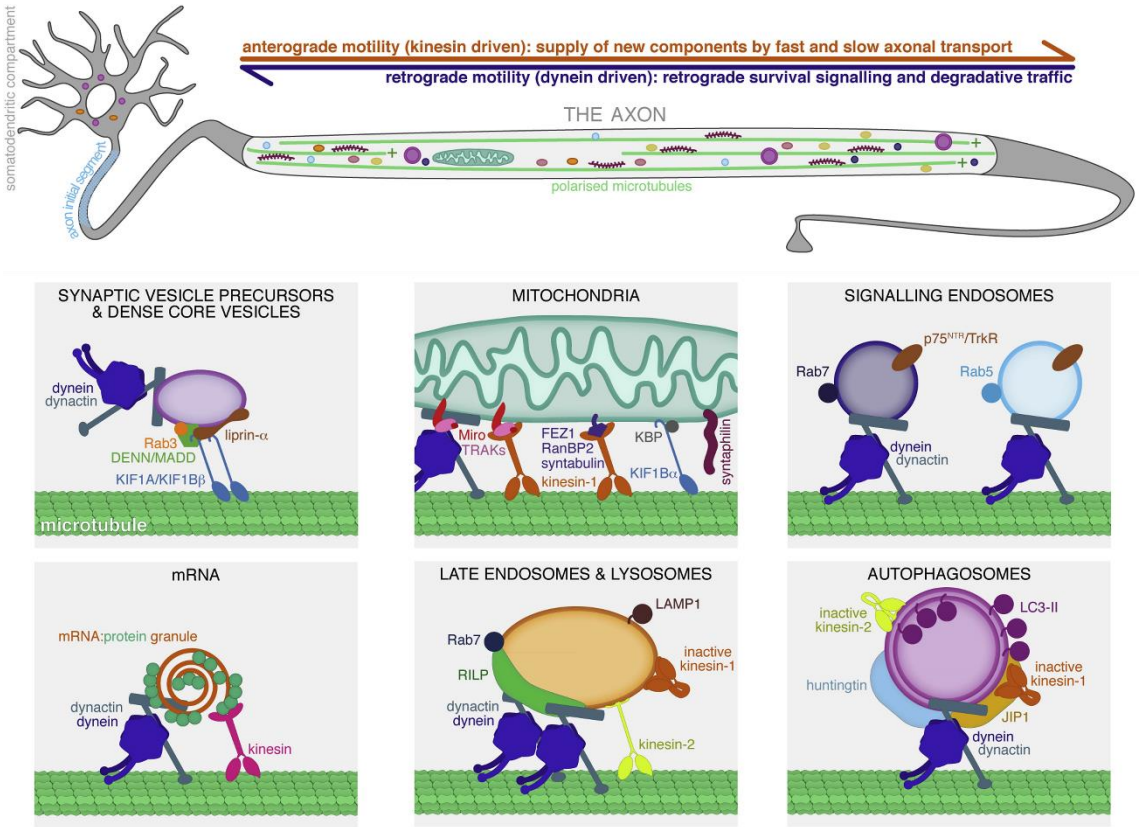

Figure 1 – Dynein and kinesins are essential for the axonal transport. The axonal transport on microtubules is regulated by the coordination between retrograde (towards the cell body) and anterograde transport (towards the tip of axon). The major motor proteins responsible for this transport are dynein and kinesin, respectively. Adapted from Maday et al., 2014.

The balance between anterograde and retrograde transport in axons is essential for the function and survival of neurons. Kinesins and dyneins are the motor proteins responsible for this transport along microtubules. Most kinesins drive axonal anterograde transport of vesicles, organelles, proteins, and RNA particles. Kinesin family 14 has a small role in the retrograde transport; however, dynein is the major motor responsible for axonal retrograde transport (minus-end directed), achieving speeds of typically 0.5–2 μm s^{-1}, in living cells (Roberts, 2018). Several cargos, including membranous vesicles and organelles such as mitochondria, move in both directions in axon, and are transported by these two motors. The regulation of the motility direction seems to be dependent on the cargo that has to be transported, but the underlying mechanisms of this regulation are still not clear understood (Hirokawa et al., 2010).

2. CYTOPLASMIC DYNEIN 1

Dynein family comprises 16 different dynein heavy chain genes in humans, which move cargos towards minus-ends of microtubules (Roberts, 2018). Most of the dynein heavy chain genes have functions within the axoneme, where they help to coordinated beating of cilia and flagella (Kardon and Vale, 2009). Only two dyneins are responsible by transport cargos along microtubules: intraflagellar (IFT) dynein and cytoplasmic dynein. IFT dynein moves cargos from the tip of the cilia towards the basal body. Cytoplasmic dynein 1 (hereafter dynein) is responsible for the minus-end directed transport within the cytoplasm, and has several additional mitotic functions (Kardon and Vale, 2009; Roberts et al., 2013).

Dynein functions include exerting pulling forces on the microtubule network that contributes to the positioning of several organelles (Roberts et al., 2013). Dynein drives the perinuclear positioning of the Golgi during interphase, and the nuclear rotation and positioning, centrosome separation and nuclear envelope breakdown in the beginning of mitosis (Figure 2). Dynein is also responsible for the minus-end directed transport of several organelles, such as endosomes, lysosomes, mitochondria, phagosomes, and lipid droplets (Figure 2). In addition, dynein has an essential role in the autophagy clearance of the cells, transporting protein aggregates to the degradative machinery usually present in the cell centre. Some studies have shown that the disruption of dynein motor blocks transport between organelles (Presley et al., 1997) and neuronal retrograde transport (Koushika et al., 2004).

Additionally, dynein has functions in mitosis where it is responsible for focusing the microtubules minus-ends at the spindle poles, stablishing the interaction between kinetochores and microtubules, inactivation of the spindle assembly checkpoint, and

finally as a pulling force on the spindle contributing for the segregation of the chromosomes at anaphase (Roberts et al., 2013).

Considering the diversity of functions driven by dynein, its spatial and temporal regulation is highly important. Several proteins, including dynactin, bicaudal D, and Hook proteins, have been described as regulators of dynein functions (Kardon and Vale, 2009; Raaijmakers et al., 2013; Liu, 2017; Redwine et al., 2017).

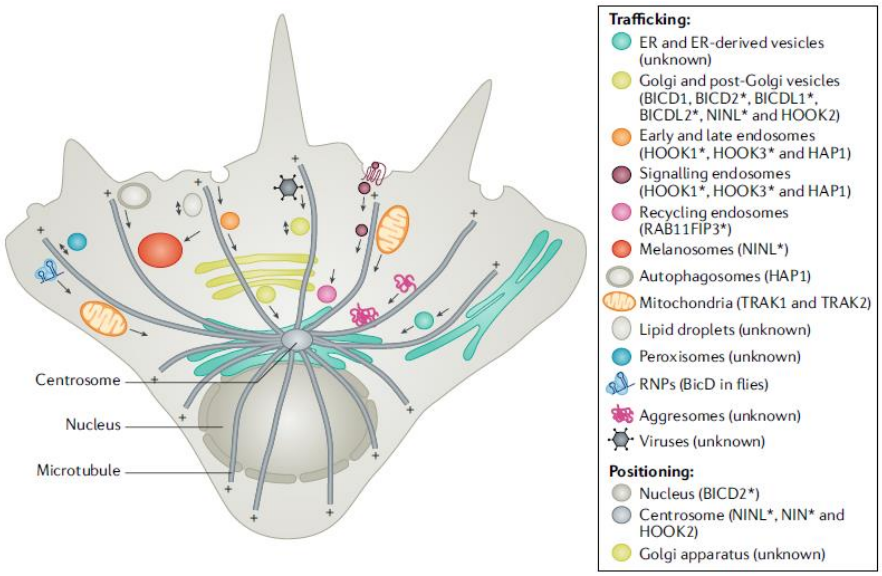

Figure 2 – Dynein complex is responsible for the organelle transport and positioning. Dynein functions include moving different cargos along microtubules towards the centrosome, and contribute to the positioning of Golgi and nucleus. This trafficking demands a high level of regulation that is not well understood. Adapted from Reck-Peterson et al., 2018.

2.1 THE STRUCTURE OF DYNEIN

Dynein forms an approximately 1.4 MDa complex, composed by a homodimer of two heavy chains (DHC). Each heavy chain is comprised of a ring of six AAA+ (ATPases associated with various cellular activities), which binds and hydrolyses ATP, a microtubule-binding domain (MTBD) at the tip of an antiparallel coiled coil (stalk) and an N-terminal tail. The tail of the dynein heavy chain is important for homodimerization and forms a platform for the binding of several noncatalytic dynein subunits: two intermediate chains (DIC), two light intermediate chains (DLIC) and three light chain (DLC) dimers [T-complex testis-specific protein 1 (TCTEX), LC8, Roadblock] [Figure 3; (Raaijmakers et al., 2013; Cianfrocco et al., 2015)].

Dynein is a processive motor moving along microtubules fuelled by ATP hydrolysis on dynein's motor domain. When MTBD is interacting with microtubules, the binding of the ATP to the motor domains leads to conformational remodelling of the

dynein complex that releases the MTBD from the microtubules. The hydrolysis reaction produce force that induces the movement of the whole dynein forward. The release of the ADP will lead to the binding of MTBD to the microtubules, and to the start of the cycle again (Cianfrocco et al., 2015).

Purified mammalian dynein has been shown to have diffuse and non-processive movements on microtubules *in vitro* (McKenney et al., 2014). The interaction between dynein and its regulators is crucial for the motor to become highly processive, moving with velocities similar to those observed in living cells (approximately 892 nm s^{-1}) (McKenney et al., 2014).

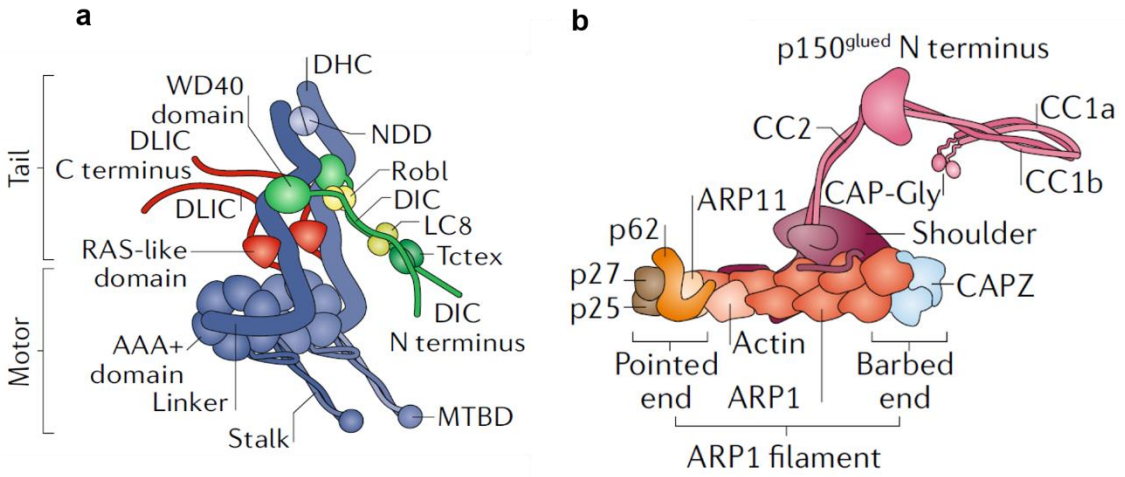

Figure 3 – Motor complex dynein and dynactin. (a) Dynein is a 1.4 MDa complex composed by two dynein heavy chains (DHC; blue) that interact with two intermediate chains (DIC; green), two light intermediate chains (DLIC; red) and three light chain (DLC; yellow) dimers [T-complex testis-specific protein 1 (TCTEX; green), LC8, Roadblock]. (b) Dynactin is a 1.0 MDa complex composed by ARP1 filament (composed by 8 ARP1 subunits; red), a barbed end (composed by CAPZ subunit; light blue), a pointed end (composed by p25 and p27 - brown, p62 - orange and ARP11 - light pink), and a shoulder composed by p50 (shoulder - violet), p24, and $p150^{GLUED}$ (pink). Adapted from Reck-Peterson et al., 2018.

2.2 THE REGULATION OF DYNEIN-DEPENDENT CARGO TRANSPORT

Dynein interacts with several proteins that are important for the processivity of the motor and for adapting the motor to its cellular function, but do not belong to the dynein complex itself.

After the discovery of cytoplasmic dynein 1 in 1987 (Paschal et al., 1987), dynactin was characterized as an essential co-factor for its activity (Gill et al., 1991; Holzbaur et al., 1991). Dynactin is 1.0 MDa complex composed by a short actin-like filament (eight copies of ARP1 and a single β-actin subunit), capped by CAPZ at the barbed end, and ARP11 at the pointed end. In the pointed end can be also found three additional subunits: p62, p25, p27. Finally, a shoulder-like domain sits near the barbed

end, and it is composed by two copies of $p150^{GLUED}$, four copies of p50 and two copies of p24. At the edge of $p150^{GLUED}$ are the CAP-Gly and the basic patch domains, which are implicated in microtubule binding (Urnavicius et al., 2015).

The deletion or inhibition of dynactin leads to phenotypes similar to the loss of function of dynein (Raaijmakers et al., 2013). Additionally, overexpression of the p50 subunit (also called dynamitin) or the CC1 fragment of the p150 subunit disrupts dynein functions (Echeverri et al., 1996; Quintyne et al., 1999). Dynactin is responsible for lowering the detachment rate of the dynein complex, increasing its processivity and enhancing its recruitment to microtubules, and for targeting dynein to specific cellular locations (Ayloo et al., 2014).

Recently, cryo-electron microscopy (cryo-EM) studies have shown that isolated dynein exists in an auto-inhibited form, called “phi-particle”. In this conformation, the motor domains are locked and have low affinity for microtubules. The formation of a ternary complex between dynein, dynactin and an adaptor protein is essential to make this motor highly processive, and release it from the autoinhibited form (Zhang et al., 2017).

Numerous proteins are being described as interactors and regulators of dynein functions. Some of these proteins, called adaptors, are known to increase dynactin affinity for dynein, and mediate the binding of the motor complex to several cargos [Figure 4; (McKenney et al., 2014)]. These adaptors are generally composed by an N-terminal region that mediates the binding to the motor complex, and a C-terminal region that links the adaptor to cargos. BICD2, SPDL1, Hook1/3, RFIP3 are known adaptor proteins promoting long distance movement of dynein-dynactin complexes (activating adaptors; Supplementary Table S1).

The cryo-EM structures of dynein-dynactin-activating adaptors (BICD2, BICDR1, and Hook3) complexes showed a common long coiled-coil characteristic in all the adaptors siting along the length of the dynactin filament (Figure 4; Urnavicius et al., 2015, 2017). Recently, BICD2, BICDL1, and Hook3 were shown to have the ability to recruit two dyneins to dynactin in order to increase the force production and speed of the complex, and allow the clustering and coupling of dynein motors for the transport of large cargos (Urnavicius et al., 2017).

Dynein transports several cargos such as endosomes, lysosomes, phagosomes, melanosomes, peroxisomes, lipid droplets, mitochondria and vesicles from the endoplasmic reticulum. Additionally, dynein is also known to be important in the transport of protein complexes or ribonucleoproteins (RNP). Several viruses (human immunodeficiency virus, herpesvirus and adenovirus) have mechanisms to hijack this motor in order to reach the nucleus.

The transport of Golgi-derived vesicles has been associated to dynein by a molecular bridge composed by dynein-dynactin complex, and BICD family adaptors. BICD family proteins contribute to several processes in the secretory pathway (Hoogenraad and Akhmanova, 2016), and are described as regulators of the endosomal sorting of neurotrophin receptors in neurons (Terenzio et al., 2014). The BICD family members are known to mediate the binding of dynein-dynactin to Rab6-Golgi vesicles (Matanis et al., 2003), as well as mRNAs (Matanis et al., 2003; Splinter et al., 2012; Gama et al., 2017).

Dynein is also required for the endolysosomal system transport in cells. Disruption of dynein function is known to disperse lysosomes and endosomes and block endosomal transport along axons (Reck-Peterson et al., 2018). Adaptors from Hook family have been implicated in the transport dynein-driven of early endosomes (Bielska et al., 2014). The late endocytic transport to degradative compartments involves the interaction of RILP, a possible dynein adaptor (Cantalupo et al., 2001). RILP is implicated in the regulation of the lysosomal morphology and distribution (Progida et al., 2007), and it is known to be associated with Rab-late endosomes and lysosomes (Jordens et al., 2001).

Dynein is also important in the transport of larger cargos such as mitochondria. In *Drosophila*, mutations in dynein heavy chain (DHC) genes alter the velocity and run length of retrograde transport in the mitochondrial axonal transport (Pilling et al., 2006). Neuronal mitochondria undergo dynamic, bidirectional transport frequently changing directions, pausing or switching to persistent docking. Only 30-40% of mitochondria are in motion, and more than half are static (Course and Wang, 2016). This organelle frequently changes direction, and usually docks in cellular places with higher metabolic demands.

The association of adaptor proteins to mitochondria is crucial for the motor attachment and mitochondrial transport. The motor–adaptor–receptor complexes ensure targeted transport of mitochondria and precise regulation of their mobility, but so far no dynein-mitochondria direct interaction was observed. Two dynactin subunits, p150^{GLUED} and p62, are known to interact with mitochondrial receptors such as Milton (TRAK1 and TRAK2 in humans) and Miro proteins (Liu, 2017). TRAK1 and TRAK2 share some homology with BICD family member, BICDR1, raising the possibility that TRAK proteins are adaptors of dynein-dynactin for the motility of mitochondria.

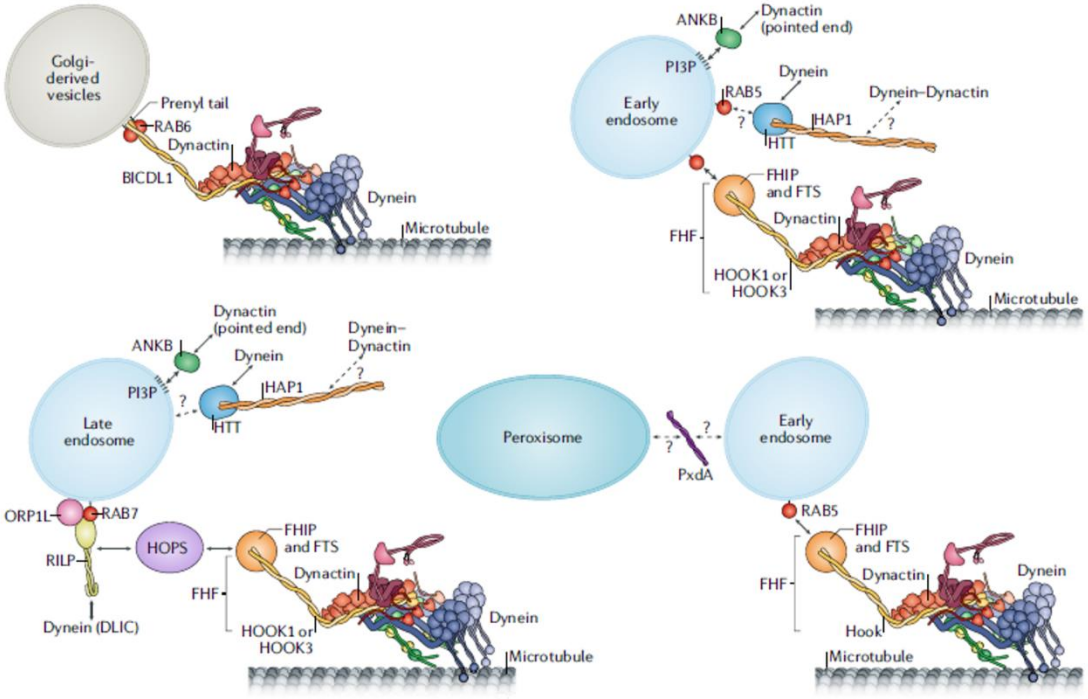

Figure 4 - Different molecular bridges that link dynein-dynactin to membrane cargos. Dynein and dynactin associate to Golgi-derived vesicles, endosomes and peroxisomes by establishing molecular bridges. DLIC may have an essential role in these bridges, interacting with several adaptors. Adapted from Reck-Peterson et al., 2018.

2.4 DYNEIN LIGHT INTERMEDIATE CHAIN AND ITS INTERACTION WITH ADAPTORS

Dynein light intermediate chain (DLIC) is a dynein subunit responsible for mediate the binding of many intracellular cargos, and it was shown to be essential for the dynein motor functions (King et al., 2002; Trokter et al., 2012).

Invertebrates contain a single DLIC gene while vertebrates have two DLIC genes (DLIC1 and DLIC2), which may define two functionally distinct dynein populations (Hughes et al., 1995). The depletion of both DLIC genes results in a severe phenotype similar to DHC depletion (Raaijmakers et al., 2013). However, the depletion of DLIC1 alone in human cells do not cause disruption, mislocalization or functional abrogation of dynein (Sivaram et al., 2009).

Knockdown studies have implicated DLIC in membrane trafficking toward the endosomal-recycling compartment (ERC) (Horgan et al., 2010), and lysosomal localization and morphology (Tan et al., 2011). Koushika et al. showed that *Caenorhabditis elegans* (*C. elegans*) DLIC orthologue, *dli-1, null* mutants have mis-accumulations of cargos in the axon terminals due to defects in the axonal retrograde transport (Koushika, 2004).

Structurally, the DLIC subunit can be divided in two different regions: one highly conserved N-terminal region that has a Ras-like domain, and one less conserved C-terminal domain. The conserved domain of DLIC is about 300 residues and makes contact with DHC (Schroeder et al., 2014). The less conserved C-terminal region is about 140 residues, and it is predicted to be disordered (Schroeder et al., 2014) with two conserved alpha-helixes - helix1 (human DLIC1 residues 440-456) and helix2 (human DLIC1 residues 493-502).

Several studies show that some of dynein known adaptors, such as Hook1/3, BICD2, NIN, RFIP3, and Spindly bind to the C-terminal region of DLIC (McKenney et al., 2014; Schroeder et al., 2014; Schroeder and Vale, 2016; Gama et al., 2017), and thus this region may be essential in the transport functions of dynein. All of these proteins are generally unrelated but share several features: a N-terminal putative binding site for the DLIC C-terminal region, a long (>200 residues) coiled-coil region, and a C-terminal binding site for proteins that link the adaptor to cargos (Reck-Peterson et al., 2018).

The binding between the adaptors and DLIC C-terminal region is mediated by different domains, such as “CC1-box” and “Hook-domain”. “CC1-box” is a short stretch of coiled coil, known to be used by BICD2, BICDL1, and Spindly to bind dynein. The “Hook-domain” was been shown to bind DLIC C-terminal region in Hook1 and Hook3 (McKenney et al., 2014; Schroeder and Vale, 2016).

The description of the interaction domains of the adaptors that link them to DLIC has led to an increase in the number of candidate activating adaptors (Supplementary Table S1). The possibility that the C-terminal region of DLIC may also offer a direct link of binding to cargo is also under investigation (Reck-Peterson et al., 2018).

A recent study identified a conserved region, helix1, of the DLIC1 C-terminal region that mediates the interaction of dynein with the adaptor proteins. In this study, isothermal titration calorimetry and crystallography were used to characterize the interaction of helix1 and the adaptor proteins Hook1/3, BICD2, and Spindly (Lee et al., 2018). The functional significance of the DLIC1 helix1 interaction with the adaptor proteins (Hook3 and BICD2) was tested by total internal reflection fluorescence microscopy (TIRF). This assay allowed to monitor the dynein-driven motility of single-molecules in the presence of helix1 or helix1$_{F447A,\ F448A}$ peptides (these point mutations were previously found to inhibit the binding of DLIC1 to the Hook-domain) (Lee et al., 2018). This assay showed that the addition of helix1 leads to a nearly complete inhibition of the motility of dynein-dynactin complex, caused by the binding of the helix1 peptide to the adaptor. This interaction prevents the binding of the dynein-dynactin complex to the adaptor. In contrast, with the addition of helix1$_{F447A,\ F448A}$, which does not bind to the adaptors, they saw motility levels similar to the control situation. This assay confirmed

that the disruption of the binding between dynein and the adaptors abrogate the motility of the motor complex. HeLa cells were also used in the same study, showing that overexpressing of DLIC with point mutations in helix1 resulted in abnormal localization of lysosomes which appeared dispersed in the cytoplasm. As suggested in the *in vitro* assays, this result confirms DLIC1 helix1 is required for processive dynein-based motility in cells (Lee et al., 2018).

In our lab, purified GST-tagged versions of DLIC1 C-terminal region were shown to bind to BICD2, Spindly, Hook3, RILP, FIP3 and Ninein. The conserved helix1 was shown to be essential for binding to adaptors. Yet, with the exception of RILP, none of the adaptors were detected in pull-downs experiments when the helix1 is alone, suggesting that additional segments in the C-terminal region are needed for efficient binding to adaptors (unpublished work from our lab).

The most recent works on dynein activating adaptors have increased the knowledge about the biochemical interactions stablished by the generally unrelated proteins with DLIC C-terminal region. Several *in vitro* studies associate these adaptors to the assembly and activation of the motor complex (McKenney et al., 2014; Schroeder and Vale, 2016; Gama et al., 2017); however, the significance of these interactions in dynein functions *in vivo* is poorly explored.

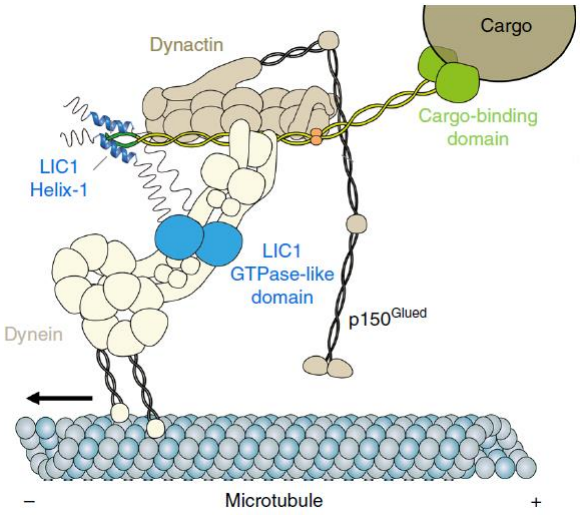

Figure 5 - Dynein light intermediate chain contributes to interaction of dynein with the adaptor. The C-terminal region of LIC is essential for the contacts with adaptor proteins that lead to a conformation of a highly processive ternary complex and mediate the binding to different cargos. Adapted from Lee et al., 2018.

3. CAENORHABDITIS ELEGANS AS A MODEL

In 1974, Sidney Brenner introduced *C. elegans* as a model to study development and neurobiology. Since then, the major molecular and cell biology protocols have been optimized, and several genetic tools emerged in order to make possible the use of this model in numerous fields, such as evolution, ecology and behaviour.

C. elegans is a transparent nematode (roundworm), whose life cycle begins with an egg stage, followed by four larval stages (L1-L4) and adulthood (AD). Reproduction of these animals occurs by self-fertilization or cross-fertilization with males. Hermaphrodites mostly compose this species; however, 0.2-1% of males may appear in worm populations.

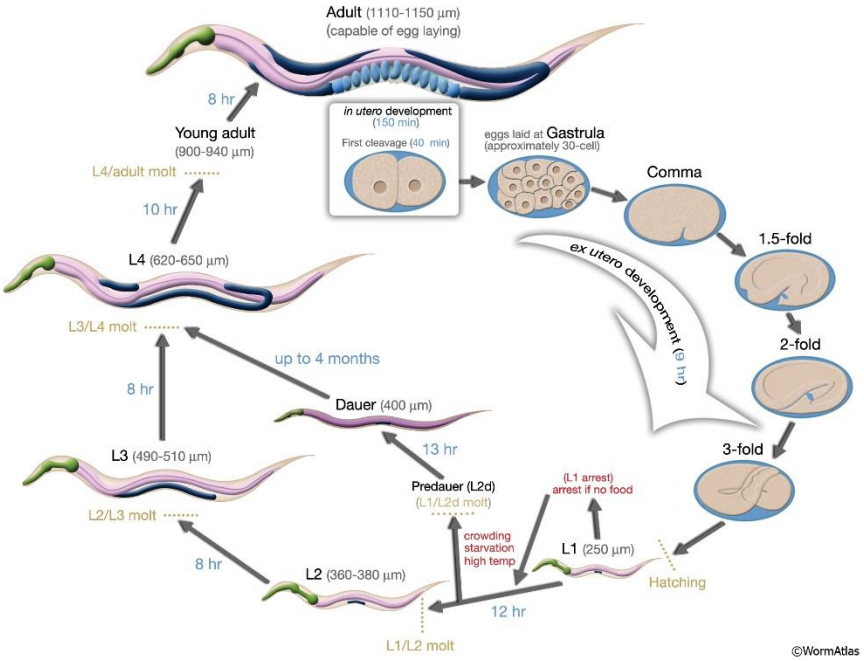

Figure 6 - *C. elegans* life cycle. Adapted from WormAtlas©.

As a multicellular organism, *C. elegans* is an ideal model system since it provides a system of several cellular differentiated tissues including muscle, neurons, reproductive system (Koushika and Nonet, 2000). However, it retains the technical simplicity associated with less complex models.

In 1998, the *C. elegans* Sequencing Consortium was able to completely sequence the genome of this nematode, becoming the first animal to have its genome fully sequenced (*Genome Sequence of the Nematode C. elegans: A Platform for Investigating Biology*, 1998). Its genome consists of 97 megabases and contains approximately 19000 predicted genes.

The major advantages of this animal model are its ability of self-fertilizing, that allow mutagenesis to be easily propagated, and its short life cycle (~3 days at 25 ºC) and

large brood size, that make possible largescale studies in a short period of time. Additionally, it is possible to establish direct extrapolation of the knowledge obtained between *C. elegans* and mammals, thanks to the conservation between numerous molecular and cellular processes.

Wormbase, a well-developed database of worm information, is also available online and includes numerous links to methods resources and user-groups.

This model has genetic versatility in the manipulation of gene expression by promoter-driven expression of stably integrated transgenes, RNAi-mediated knockdown, or gene mutations. These mutagenesis techniques are highly used and described in *C. elegans*, being described several protocols and strategies for directed mutagenesis (Chen et al., 2013; Dickinson et al., 2013; Ran et al., 2013; Xu, 2015).

In addition to its availability for strong genetic techniques, *C. elegans* has proven useful for both biochemical and cell biological approaches. In systematic screens, all predicted genes have been silenced using RNAi, and several databases where created with siRNA's used and resulting phenotypes (*C. elegans RNAi Collection – Ahringer; PhenoBank Project*).

In cell biology studies, its transparent cuticle and thin body allow the visualization of all cells, and the use of fluorescently labelled proteins and vital dyes within the living organism (Koushika and Nonet, 2000).

3.1 TOUCH RECEPTOR NEURONS AS A MODEL TO STUDY AXONAL TRANSPORT

C. elegans has proven to be a powerful model in neurobiology studies since it has a precise neuronal anatomy that is predetermined and has one of the simplest nervous systems described. In hermaphrodites, the nervous system is composed of 302 neurons. In 1986, the detailed wiring diagram of the neural circuits was published, and since then this model has been used in several neurobiology studies (White et al., 1986). The touch receptor neurons (mechanossensory neurons) are the most used to study neuronal trafficking.

There are six touch receptor neurons along *C. elegans* body. Three of them are found in the interior part of the animal (AVM, ALML, ALMR) and three in the posterior part (PVM, PLML, PLMR). This set of neurons is responsible for the response to gentle touch. The touch-response circuit involves other sets of neurons (interneurons and motor neurons). The processes of touch receptor neurons act both as dendrites receiving the touch stimulus and as axons carrying the signal to downstream neurons.

In *C. elegans*, the processes of mechanosensory neurons have microtubules with a larger diameter (15-protofilament), organized with the plus-ends towards the axon terminals and the minus-end towards the cell body (Chalfie and Thomson, 1979; Martin

Chalfie, 1990). The mechanosensory neurons are the most used neurons to study axon dynamics, since have well defined processes, and are the closest neurons to the animal's cuticle.

These neurons are easily identified by expression of reporter genes controlled by *mec-7* and *mec-4* promotors. The use of reporter genes, such as GFP or mKate2, allows the study of neuron morphology and localization. Several studies have been published referring to the study of axonal cargo transport and distribution (Koushika, 2004; Sure et al., 2018).

In these cases, the most used experimental approach is to label specific cargos with fluorescent proteins under the control of histospecific promotors, such as *Pmec7* and *Pmec4*. The construction of a *C. elegans* strain where is possible to co-localize neuronal processes and cargos allow the study the dynamics of neuronal transport.

The acquisition of appropriate *in vivo* data for this type of biological process is a challenge. The most used tools to study these dynamic processes are high-resolution time-lapse imaging, and confocal imaging of fluorescently labelled cargos in neuron segments. The two approaches can be used to study the axonal motility of cargo (Koushika et al., 2004; Arimoto et al., 2011; Sood et al., 2018; Sure et al., 2018).

The improvement of the imaging technology, and of data analysis algorithms are leading to the expansion of these techniques and making easier the comprehension of the biological significance of the data (Mondal et al., 2011; Nair et al., 2014; Alloatti et al., 2018).

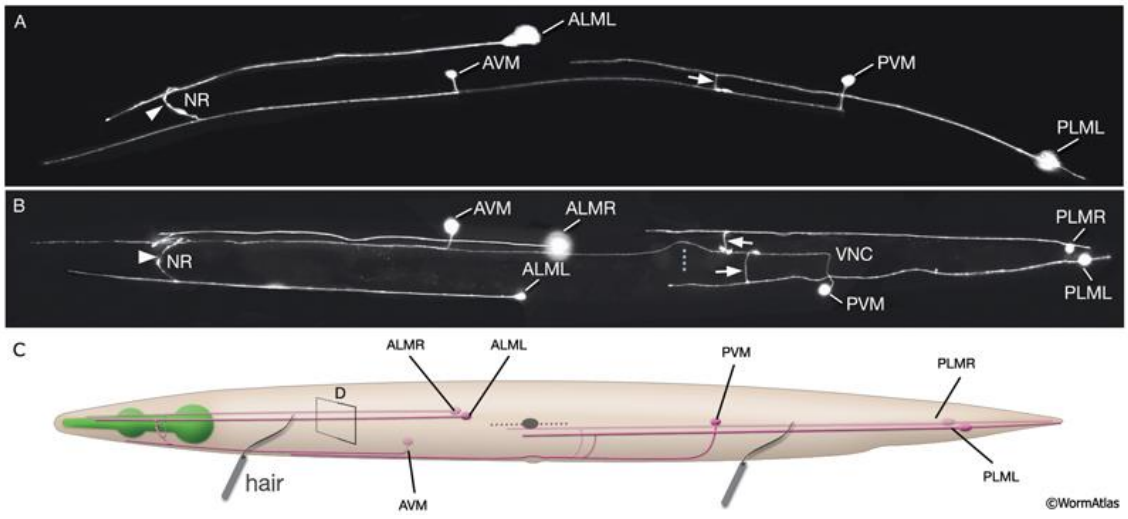

Figure 7 - Mechanosensory neurons that sense gentle touch, expressing the reporter gene mec-4::GFP. A) Left lateral view; B) Ventral view; C) Graphic rendition of touch receptor neurons as seen from the left side. Adapted from WormAtlas©.

II. AIMS OF THE STUDY

Several neurodegenerative diseases are associated with defects in axonal transport. Dynein, a well-known motor protein, is responsible for the retrograde microtubule-based transport and several studies show that the dynein subunit DLIC binds to cargo adaptor proteins. In our lab, protein-binding assays showed that the DLIC1 C-terminal region is essential for the binding to the adaptors BICD2, Spindly, Hook3, RILP and Ninein. Additional, four point mutations in the conserved helix1 resulted in the disruption of this binding, suggesting a crucial role for this helix.

The aim of this study is to explore the role of the described interaction between DLI-1^{helix1} and the adaptors in *C. elegans* axonal transport. This contribution will increase the knowledge regarding the interactome of dynein and its regulation. The perturbation of dynein complex and its close relationship with neuronal transport defects will also increase the knowledge in neurodegenerative diseases and processes. Considering the major aim described, three fundamental tasks were established:

1. Direct mutagenesis in the conserved helix-1 of *C. elegans* DLI-1 C-terminal region by CRISPR-Cas9 technology. The mutations inserted were previously shown to prevent DLIC binding to cargo adaptor *in vitro* (unpublished results from our lab) and affect lysosome transport in cells (Lee et al., 2018);
2. Detailed description of morphological phenotypes, longevity and motility associated to the inserted mutations in the animals;
3. Evaluate the relevance of the adaptor-DLIC helix1 interaction for the transport of diverse cargos. The identification of cargo mis-accumulations at the tip of the axons in the touch receptor neurons of *C. elegans* indicates the disruption of the retrograde transport (Koushika et al., 2004).

III. MATERIAL & METHODS

1. CAENORHABDITIS ELEGANS STRAINS

The wild-type N2 strain (Bristol ancestral) and the balancer strain (VC362) from *C. elegans*, as well as *Escherichia coli* OP50 bacteria, were obtained from the *Caenorhabditis* Genetics Center (CGC), a central repository for strains under contract from the NIH National Center for Research Resources (http://biosci.umn.edu/CGC/CGChomepage.htm).

The Table 2 lists all strains used in this study, and their respective genotype.

The worm strains are maintained at 20ºC on Nematode Growth Medium (NGM) agar petri plates seeded with OP50 bacteria. OP50 is a uracil auxotroph with a slower growth rate than wild-type *E. coli* and is not resistant to antibiotics. Preparation of plates is as mentioned on WormBook.

Strains were cryopreserved at -80ºC, in order to keep them available at any time.

Table 2 - List of all strains that were required for the study.

	STRAIN	GENOTYPE
Wild-type	N2	WT (ancestral N2 Bristol)
	GCP302	unc-119(ed3) III; prtSi99[pRG525; 0.85 kb mec-7 5'UTR::tomm-20(aa 1-54)::mKate2::tbb-2 3'UTR; cb-unc-119(+)] II; zdIs5 [Pmec-4::gfp + lin-15(+)] I
	GCP311	unc-119(ed3) III; prtSi104[pRG527; 0.85 kb mec-7 5'UTR::mKate2::rab-5::tbb-2 3' UTR; cb-unc-119(+)] II; zdIs5 [Pmec-4::gfp + lin-15(+)] I
	GCP330	unc-119(ed3) III; prtSi101[pRG526; 0.85 kb mec-7 5'UTR::snb-1::mKate2::tbb-2 3'UTR; cb-unc-119(+)] II; zdIs5 [Pmec-4::gfp + lin-15(+)] I
DLI-1 mutants	GCP611	dli-1[prt96(Δaa369-443)]IV; IV/nT1[qIs51];V/nT1[qIs51](IV/V)
	GCP671	dli-1[prt106(F392A/F393A)]IV; IV/nT1[qIs51];V/nT1[qIs51](IV/V)
	GCP672	dli-1[prt107(L396A/L397A)]IV; IV/nT1[qIs51];V/nT1[qIs51](IV/V)
	GCP673	dli-1[prt96(Δaa369-443)]IV; IV/nT1[qIs51];V/nT1[qIs51](IV/V); unc-119(ed3) III; prtSi104[pRG527; 0.85 kb mec-7 5'UTR::mKate2::rab-5::tbb-2 3' UTR; cb-unc-119(+)] II; zdIs5 [Pmec-4::gfp + lin-15(+)] I
	GCP679	dli-1[prt106(F392A/F393A)]IV; IV/nT1[qIs51];V/nT1[qIs51](IV/V); unc-

	119(ed3) III; prtSi104[pRG527; 0.85 kb mec-7 5'UTR::mKate2::rab-5::tbb-2 3' UTR; cb-unc-119(+)] II; zdIs5 [Pmec-4::gfp + lin-15(+)] I
GCP680	dli-1[prt107(L396A/L397A)]IV; IV/nT1[qls51];V/nT1[qls51](IV/V); unc-119(ed3) III; prtSi104[pRG527; 0.85 kb mec-7 5'UTR::mKate2::rab-5::tbb-2 3' UTR; cb-unc-119(+)] II; zdIs5 [Pmec-4::gfp + lin-15(+)] I
GCP696	dli-1[prt107(L396A/L397A)]IV; IV/nT1[qls51];V/nT1[qls51](IV/V); unc-119(ed3) III; prtSi101[pRG526; 0.85 kb mec-7 5'UTR::snb-1::mKate2::tbb-2 3'UTR; cb-unc-119(+)] II; zdIs5 [Pmec-4::gfp + lin-15(+)] I
GCP697	dli-1[prt107(L396A/L397A)]IV; IV/nT1[qls51];V/nT1[qls51](IV/V); unc-119(ed3) III; prtSi99[pRG525; 0.85 kb mec-7 5'UTR::tomm-20(aa 1-54)::mKate2::tbb-2 3'UTR; cb-unc-119(+)] II; zdIs5 [Pmec-4::gfp + lin-15(+)] I

2. GENOME EDITING IN *C. ELEGANS*

The sequence alignment of the C-terminal disordered region in the two human DLIC paralogs and the sole DLIC orthologue in *C. elegans*, DLI-1, was done to identify the position of the highly conserved residues in helix1 that are required for binding to adaptors *in vitro*. Three strains were constructed: a strain with a deletion of the entire DLI-1 C-terminal region from residue 369 to 443 (Δ369-443); and two strains mutating four conserved residues in the helix1 of DLI-1 C-terminal region: phenylalanine 392 and phenylalanine 393 to alanines (F392A/F393A), and leucine 396 and leucine 397 to alanines (L396A/L397A).

2.1 CRISPR-CAS9 CO-CONVERSION STRATEGY

The type II CRISPR-Cas9 system is a powerful tool for genome editing in a variety of experimental systems, including *C. elegans*. Even though this system is based on a prokaryote model, it is easy to express endonuclease Cas9 in the nematode's germline by injecting an expression plasmid (Dickinson et al., 2013).

CRISPR-Cas9 works by the Cas9 recognition of the cleavage site that leads to a double-strand break site that will be repaired allowing the addition of a repair template containing the desired mutations (deletions, insertions or point mutations).

In CRISPR-Cas9 genome editing strategy, single-guide RNAs (sgRNAs) guide the Cas9 to the target site by recognizing in the genome, a protospacer adjacent motif

(PAM) (NGG for Streptococcus pyogenes Cas9) and a region of 20 bp of complementarity to its sgRNA. After that, the double-strand break made by Ca9 can be repaired via Non-Homologous End-Joining (NHEJ) or by a Homologous Repair mechanism from a template or donor DNA (HR) (Rok and Yup, 2016).

It is important to have in consideration the number of off-targets sites of Cas9 that the sgRNA can generate, and the proximity of these off-targets to the desired modification. These considerations were based in previous optimization and parameters mentioned in other works (Ran et al., 2013; Arribere et al., 2014; Dickinson and Goldstein, 2016).

The co-conversion strategy used in our lab is important when the desired mutation does not result in a readily identifiable phenotype. This strategy is based on the addition of a second unlinked mutation by the same CRISPR-Cas9 process that results in a dominant phenotype (Arribere et al., 2014). This technique facilitates the identification of animals that were successfully exposed to Cas9, sgRNA and repair templates. Selecting only these animals might enrich the population of positive animals for the desired and unmarked mutation (Arribere et al., 2014).

All of the *in silico* process was done using bioinformatics tools [selection of sgRNA using online CRISPR Design Tool http://crispr.mit.edu/; SnapGene software (GSL Biotech, Chicago, IL, USA)].

2.1.1 sgRNA CLONING

The first phase of the process is the annealing of two oligonucleotides producing the sgRNAs. The single-stranded oligonucleotides for the selected sgRNAs construction consist in 19 nucleotides plus sticky-ends for cloning into the modified pDD162 sgRNA plasmid (listed into the Table S2), and were ordered from Sigma-Aldrich (St Louis, MO, USA). The single-stranded primers were assembled in an annealing reaction [1 µL 10xT4 DNA ligase buffer (50 mM Tris-HCl, 10 mM $MgCl_2$, 1 mM ATP, 10 mM DTT), 1 µL T4 Polynucleotide Kinase (PNK), 1 µL forward primer (100 µM), 1 µL reverse primer (100 µM) and 6 µL H_2O] in a thermocycler, using the following parameters: 37 ºC for 30 minutes, 95 ºC for 5 minutes and then a ramp down to 25 ºC at 5 ºC/min.

The pDD162 plasmid (containing a Cas9 endonuclease-codifying sequence) was previously modified in our lab by introducing two artificial BveI restriction sites flanking the sgRNA insertion site. The empty modified plasmid pDD162 was digested with BveI enzyme giving rise to a fragment with 8109 bp with overhangs (fragment of interest) and another one with 1629 bp.

The cloning of the of the double-stranded sgRNA annealing products into the modified pDD162 was performed in a reaction consisting of digested pDD162 modified

vector, a 1:200 dilution of the double-stranded sgRNA annealing products, 10x T4 DNA ligase buffer, T4 ligase and distilled H_2O. The ligation reaction was performed at 20 ºC for 2h, and then T4 DNA Ligase was inactivated at 65 ºC for 10 min.

The ligation product was added to competent DH5-α bacteria and then incubated on ice for at least 15 minutes. After that period, bacteria was submitted to a heat shock at 42 ºC, for 1 min, and right after placed on ice for 2 minutes to cool down. Bacteria were allowed to recover in 450 µl Super Optimal broth with Catabolite repression (SOC) medium, for 2h at 37 ºC with agitation. After this incubation period, bacteria suspensions were centrifuged at 850 x g, for 3 min and the supernatant was discarded. The remaining pellet was resuspended and plated on LB plates with 100mg/mL ampicillin and then cells was left to grow at 37 ºC for 16h.

The following day, colonies were picked into LB medium containing 100 mg/mL ampicillin and grown overnight at 37 ºC. Plasmid DNA was purified with the NucleoSpin® Plasmid Mini Prep Kit (Macherey-Nagel, Düren, Germany), and further confirmed by Sanger sequencing (GATC Biotech, Constance, Germany).

After obtaining sgRNAs targeting the genomic sites near the desired modification, repair templates were designed to allow the modification of a specific genomic region. The repair templates also include several silent point mutation that confer resistance to the sgRNA, and restriction sites when needed for mutational screening. Single-strand repair templates (ssODNs) with 50-60 bp homolog arms was designed in SnapGene software (GSL Biotech, Chicago, IL, USA), and ordered from Integrated DNA Technologies (IDT, Leuven, Belgium).

After gathering the specific sgRNAs plasmids and respective repair templates, an injection mix was assembled together with dpy-10 gRNA plasmid (pJA58) and dpy-10(cn64) repair oligonucleotide (Table 3). The dpy-10 gRNA plasmid and repair oligonucleotide will be responsible for a dominant roller phenotype associated to the co-conversion strategy.

2.1.2 Injection of the N2 worms to generate mutant strains

The wild-type N2 early adult animals were injected in the gonad with the mix previously described, containing a plasmid that will allow the action of the Cas9 enzyme, the incorporation of the repair templates containing the desired mutations, and the incorporation of a mutation that allow the selection of mutated worms. The injection was performed using an inverted microscope microinjection setup.

Table 3 - Composition of the CRISPR-Cas9 co-conversion injection mix.

COMPONENTS	DESCRIPTION	CONCENTRATION
pJA58	sgRNA plasmid for dpy-10 modification	25 ng/µL
dpy-10(cn64) repair template	ssODN repair template for dpy-10 modification	500 nM
sgRNA	sgRNA plasmids for the desired modification	50 ng/µL
Repair template	ssODN repair template for desired modification	50 ng/µL

Three animals per plate (F0) were grown for 3-4 days at 25ºC after injection, and transgenic progeny (F1) will selected based on the roller phenotype.

The screening strategy to assess the mutational status of the F1 animals was done by PCR (Polymerase Chain Reaction) for the DLI-1 Δ369-443 mutants, and PCR-RFLP (PCR – Restriction Fragment Length Polymorphism) for DLI-1 F392A/F393Aand DLI-1 L396A/L397A mutants, using designed oligonucleotides and restriction enzymes that recognize the point mutations inserted (Table S2; Table 4).

PCR parameters for the three mutants were as follow: 92 °C for 5 min, 10 touchdown cycles at 92 °C for 30s, 63-53 °C (-1 ºC per cycle) for 30 s and 72 ºC for 30s, followed by 25 cycles at 92 °C for 30s, 53 °C for 20 s and 72 ºC for 20s, and finally 72 ºC for 5 min.

Regarding the DLI-1 L396A/L397A and F392A/F393A animals, the restriction enzymes used were EaeI (New England Biolabs Inc., Ipswich, MA, USA), and BglI (Thermo Fisher Scientific, Walthan, MA, USA), respectively.

The digestion and PCR products were run in 2% agarose's gel and visualized at Gel Doc™ XR+ Imaging System (Bio-Rad Laboratories, Hercules, CA, USA) (Table 4). This protocol was followed in every mutational screening needed.

Table 4 - Mutational screening strategy.

MUTATION TESTED	AMPLICON (BP)		
	WT	**Heterozygous**	**Homozygous**
dli-1 Δ369-443	731	731 and 474	474
	RESTRICTION PATTERN (BP)		
	WT	**Heterozygous**	**Homozygous**
dli-1 F392A/F393A	252	252, 167, and 85	167 and 85
dli-1 L396A/L397A	220	220,151, and 69	151 and 69

2.1.3 GENETIC CROSSES

After getting positive animals for the desired mutations after the injection, the strains were crossed six times with the wild-type N2 strain in order to clean the background genome from potential off-target mutations, and the presence of the desire modifications was confirmed by Sanger sequencing (GATC, Constance, Germany).

Since the desired mutation in homozygosity lead to sterility, all the outcrosses had to be done with heterozygous animals. The first outcross was done by mating hermaphrodite animals L4-stage from a progeny of a heterozygous mother (mut+/wt) with N2 males, overnight at 25ºC. Next day, the mutational status of the mothers mated was assessed. In the plates with mother heterozygous (mut+/wt) and with males in progeny, the male's progeny was selected for the following outcrosses. These outcrosses were done by mating a male (wt/wt ; mut+/wt) from a positive plate with a hermaphrodite animal L4-stage N2, overnight at 25ºC. Next day, the mutational state of the males was assessed and so on for more five times. The mutational screening during the outcrosses was done as previously described.

The new strains are maintained using a GFP-marked balancer (strain VC362), in order to easily identify the mutants. Since homozygous worms for the three mutations described are sterile, it is not possible to propagate the strain as homozygous.

The balancer strain used aims to facilitate the identification of homozygous mutant worms, and the propagation of only-mutated worms by not enabling the growth of homozygous wild-type worms. VC362 has mutations on chromosome IV that when in both alleles (bal+/bal+) are lethal for the worm ("bal"corresponds to balancer strain allele with mutations in chromosome IV). When in one of the alleles (bal+/wt) labels the animal pharynx with GFP, and when no allele is present (wt/wt) the worm has a pharynx lacking the GFP fluorescence.

Since the mutated gene *dli-1* is also on chromosome IV when the *dli-1* mutants are crossed with this balancer strain we get a progeny with: homozygous *dli-1* mutants (mut+/mut+) that lack the GFP fluorescence and are sterile; heterozygous *dli-1* mutants (bal+/mut+) that have GFP fluorescence in pharynx and are viable; homozygous dli-*1* (bal+/bal+) that do not develop.

This strategy enables the propagation of the desired mutations and to easily identify the homozygous mutant animals by the lacking of GFP fluorescence.

Finally, in order to study axonal retrograde transport, we used strains already constructed in the lab. These previously constructed strains allow simultaneous visualization of neuronal morphology (soluble GFP expressed from the mec-4 promotor)

and early endosomes (mKate2::RAB-5 expressed from *the mec-7* promotor), synaptic vesicles (SNB-1::mKate2 expressed by *mec-7* promotor), and mitochondria (tTOMM-20(1-54)::mKate2 expressed by *mec-7* promotor). These strains were crossed with the *dli-1* mutants, following the same crossing protocol as described.

The list of all the strains used in this project is presented in *Table 2*.

3. IMMUNOBLOTTING

To test DHC-1 protein levels between the three new strains, 100 adult animals of each strain were collected to M9 buffer. After centrifugation at 600g, the pellet went through several washes with M9 buffer followed by 0.05% Triton X-100 (prepared in M9). To the left supernatant, it was added 4x SDS-PAGE sample buffer and glass beads. Samples were boiled for 3min at 95ºC and then vortexed for 5min, in a Multi-Vortex V-32 at maximum speed, twice. After centrifugation at 20 000g, for 1min, at room temperature, supernatants were collected, and kept at - 80ºC until use. Protein extracts was resolved on 7.5% SDS/polyacrylamide gels and transferred to a 0.2 µm nitrocellulose membrane (Hybond ECL, Amersham Pharmacia Biotech, Buckinghamshine, United Kingdom) using a in a Bio-Rad transfer apparatus (Bio-Rad Laboratories, Hercules, CA, USA), according to the manufacturer's instructions.

Transferred proteins were confirmed by ponceau staining (0.25% Ponceau S in 40% methanol and 15% acetic acid). Membranes were rinsed in Tris-buffered saline solutions and left in blocking buffer [5% nonfat powdered skim milk (w/v) in Tris-buffered saline solution with 0.05 % Tween 20 (v/v) (TBST)] for nonspecific sites to be blocked.

Membranes were then incubated with primary antibodies: rabbit anti-DHC-1 antibody GC4 (1:1400, made in house) and mouse monoclonal anti-α-tubulin antibody, clone B512 (Sigma Aldrich, 1:5000) overnight, at 4°C. In the following day, membranes were washed with TBS-T and incubated with the secondary antibodies [anti-rabbit IgG peroxidase polyclonal antibodies (1:5000) (Jackson Immuno Research, Suffolk, UK)] for 1h at room temperature. All antibodies were diluted in blocking buffer.

Following three washes in TBST (10min each), blots were visualized by chemiluminescence using Pierce ECL Wester Blotting Substract reagents (Thermo Scientific, Rockford, IL, USA) and x-ray film, according to the supplier's instructions.

4. LONGEVITY ASSAY

Animals were synchronized with the same egg laying day by selecting L4 animals and let them lay eggs for 8 hours. After laying the eggs, the early-adults were killed and plates were maintained in ideal conditions: NGM plates with OP50, 20ºC (Sutphin and Kaeberlein, 2009; Raj et al., 2014). When the animals grew to L4 stage, they were

selected, and placed in new plates. To prevent bacteria from been depleted, the animals were transferred to new plates twice a week. The number of death animals were scored every 1-3 days. An animal was scored as dead if it fails to respond to gentle prodding with platinum wire pick and if pharyngeal pumping is not observed. Animals were excluded if they were found dead on the edge of the plate, escaped, ruptured, or suffered from internal hatching.

5. MOTILITY ASSAY

The motility of early adults hermaphrodites (AD1) lacking GFP-fluorescent in the pharynx (mut+/mut+) was analyzed by the liquid trashing assay. The liquid trashing assay measures the frequency of movement of the animal in liquid medium. L4 animals were transferred on a new NGM plate with bacteria 16h before performing the assay. Animals were placed in a drop of M9 buffer, the animal movements were tracked using a system that consists of a SMZ 745T stereoscope (Nikon) mounted with a QIClic CCD camera (QImaging) controlled by Micro-Manager open source microscopy software acquiring 40 frames per second ImageJ plugin "wrMTrck", making the counting more precise. The ImageJ plugin counted the number of trashes (a swing from its head and tail to the same side) during 1 minute. The assay was done at 20 ºC.

6. IMAGING

AD1 animals lacking GFP-fluorescent in the pharynx (mut+/mut+) were used to evaluate worms with completely developed neuronal system but without the neuronal defects associated with aging. The age synchronization of these animals were assured by collecting them as L4 in the day before imaging. Right before imaging, worms were immobilized with sodium azide 50mM, and mounted onto 2% agarose pad.

All of the imaging protocols were performed in an inverted fluorescent Wildfield Zeiss® Axioobserver 200M Microscope (Zeiss, Oberkochen, Germany) equipped with an Orca Flash 4.0 camera, a HXP 200C light source and ZEN software (Zeiss). Köhler illumination was always adjusted before the start of every session using the elected objective for the experiment.

The morphological study of the DLI-1 mutants was done using the microscope described above. It was used the DIC Transmission Light Channel (DICII TL) with DICIII Condenser, the oil objective 40x, with 6.00V of voltage and 100ms of exposure time. It were record frames with z-stacks (step-size 5.0 µm) variation, and 1 x 1 binning.

The whole-body images were taken using the stitching tools (fuse tiles with correct shading with reference) from Zeiss software.

The axonal retrograde transport of early endosomes and synaptic vesicles in mechanossensory neurons was studied using a protocol described by Koushika et al., 2004. In this protocol, the tip of the ALM neurons and nerve ring in the anterior part of the animal were focus. The oil objective 63x was used for imaging the strains with labelled early endosomes and synaptic vesicles. The strain with labelled mitochondria was imaged with the oil objective 40x, and the focus was the whole ALM neuron (soma and axon).

In both protocols was used a 1x1 binning, GFP was excited at 488 nm and mKate was excited at 561 nm. Sequential snaps with GFP channel (exposure time of 50 msec), mKate channel (exposure time of 200 msec), and DICII TL channel were taken for each animal. In these sessions, frames with z-staks (step-size 1.0-2.0µm) variation were also record. All imaging assays were performed at a room temperature of 20ºC.

7. Data Analysis

The analysis of all the data obtained with the experiments described allowed a better understanding of the differences between the wild-type and *dli-1* mutants. The results from the longevity and motility assays were analyzed with the software GraphPad Prism7 (GraphPad software, San Diego, California, USA). In the locomotion assay, statistical significance was determined by one-way ANOVA on ranks (Kruskasl-Wallis nonparametic test) followed by Dunn's multiple comparison test.

Regarding the quantification of mKate2::RAB-5, SNB-1::mKate2, and TOMM-20(1-54)::mKate2 distribution, the image analysis was performed using the free image processing software Fiji (Image J version 1.52d, Open source software, NIH, Bethesda, Maryland, USA), available to download at https://fiji.sc/.

After maximum intensity projection of appropriate GFP z-stacks, mKate2 fluorescence intensity were recorded from the first 20µm of axonal tip (mKate2::RAB-5 and SNB-1::mKate2). The mean fluorescence intensity of the background close to the axonal tip was measured and subtracted from the mKate2 signal. For TOMM-20(1-54)::mKate2, number and distribution of mitochondria (mKate2 signal) along the ALM axon and the length of each ALM axon were recorded.

The data obtained by these quantifications was statistically analyzed using GraphPad Prism7 (GraphPad software, San Diego, California, USA). Statistical significance was determined by one-way ANOVA on ranks (Kruskal-Wallis nonparametric test) followed by Dunn's multiple comparison test.

IV. RESULTS

The morphology and development of the animals are severally affected by mutating the helix1 of DLIC^{DLI-1}.

To determine the *in vivo* significance of the C-terminal region of DLIC, the *C. elegans* orthologue *dli*-1 was mutated using CRISPR-Cas9 technology. Three mutant strains were studied: a strain depleting the entire DLIC C-terminal region from residue 369 to 443 (Δ369-443), and two strains mutating to four conserved residues in the helix1 of DLI-1 C-terminal region: phenylalanine 392 and phenylalanine 393 to alanine's (F392A/F393A), and leucine 396 and leucine 397 to alanine's (L396A/L397A). The three described mutations lead to the sterility of the animals and the strains had to be propagated balanced.

By differential interference contrast microscopy, we assessed morphological defects in homozygous mutant animals at day 1 of adulthood (AD1). The three mutants share a characteristic morphological phenotype: slightly dumpy body with a disorganized gonad architecture, protruding vulva, and aberrant structures suggestive of widespread cell death (Figure 8 and 9). This phenotype is reminiscent to the phenotype described in null mutants of *dli-1* and *dhc-1* (Koushika et al., 2004).

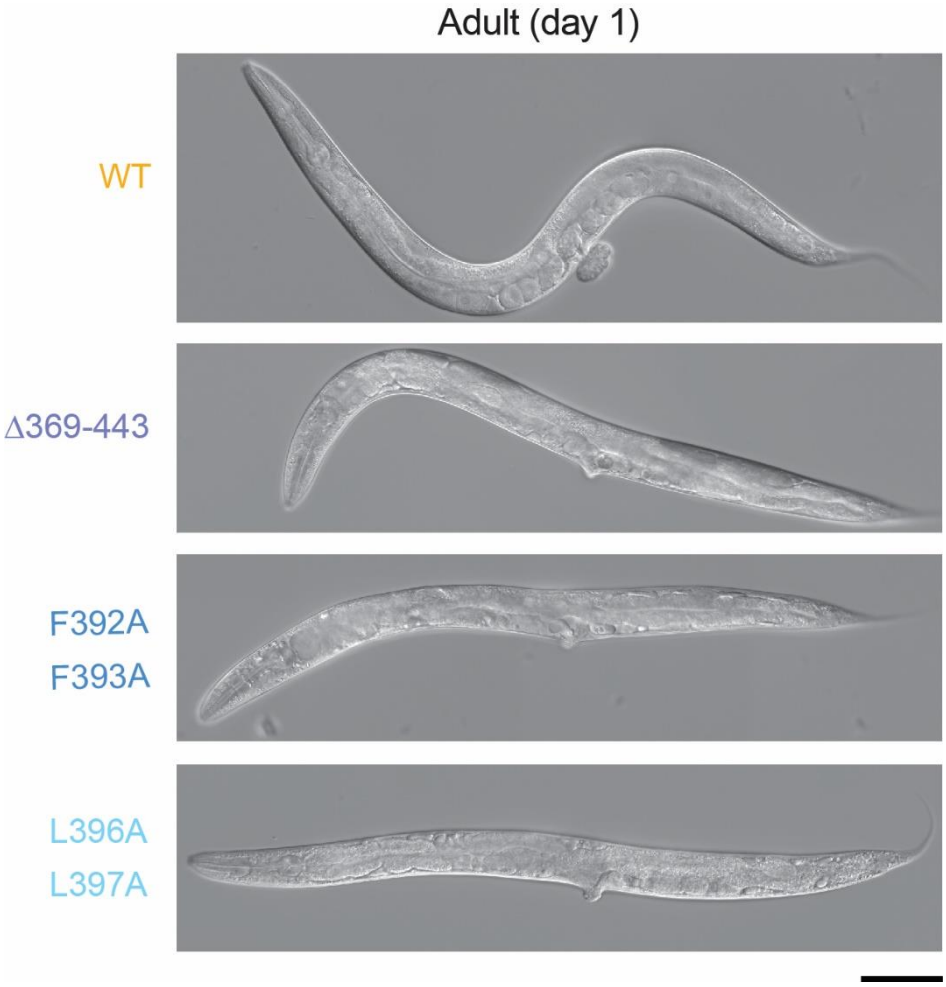

Figure 8 – Differential interference contrast microscopy of AD1 animals, showing morphological defects in *dli-1* mutants. Scale bar: 100 µm.

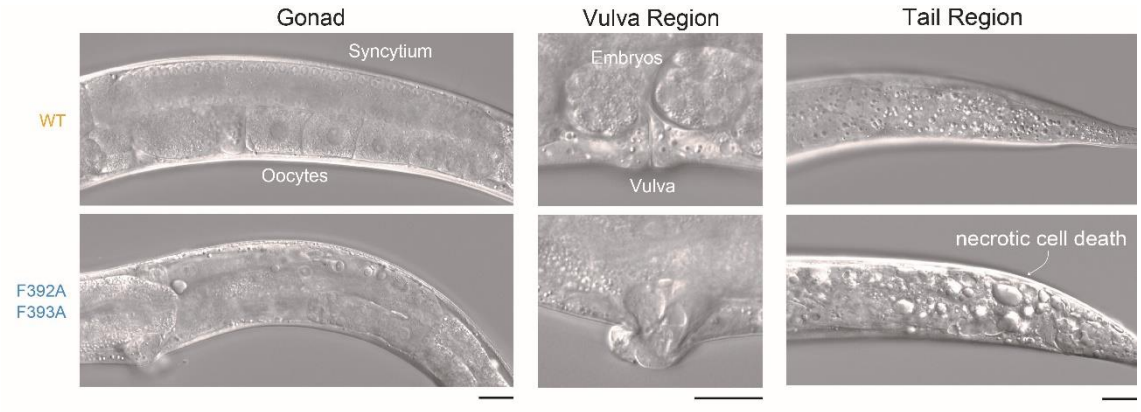

Figure 9 - Differential interference contrast microscopy in F392A/F393A mutants. This phenotype is similar to the one observed in Δ369-443 and L396A/L397A mutants. Scale bar: 20 µm.

Since mammalian DLIC is essential for dynein heavy chain stability, these phenotypes could rise from lower protein levels of dynein. By immunoblot, we assessed DHC-1 levels in the *dli-1* mutants. Protein expression of DHC-1 is not decreased, and as can be seen at Figure 10, the levels of DHC-1 appear to be slightly increased in our mutants.

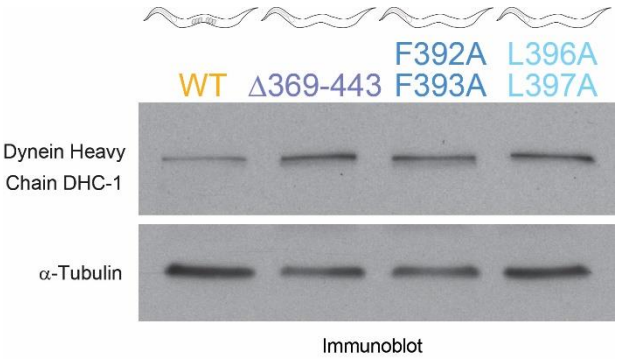

Figure 10 - Immunoblot showing levels of dynein heavy chain (DHC-1) in adults of dli-1 mutants. α-Tubulin is used as a loading control.

The mutations in the conserved helix1 of C. elegans* DLIC^{DLI-1} *lead to a decrease of longevity of the animals.

Several neurodegenerative diseases are associated with premature aging caused by the severe neurodegeneration that characterize these diseases. In order to assess if the *dli-1* mutations affect the longevity of the animals, we have done a life span assay. This assay consists in counting the number of days an animal is responsive to external stimuli.

In synchronized animals, we notice that homozygous *dli-1* mutant animals have a significantly shorten life span. The wild-type animals live 18±0.74 days, Δ369-443 animals living 13±0.39 days, F392/F393 animals living 12±0.47 days, L396A/L397A animals living 13±0.48 days (mean life span ± SEM). Moreover, at day 15 of adulthood less than 50% of the *dli-1* mutants are alive, while approximately 80% of the wild-type are alive. While some wild-type animals live up 32 days, none of the mutated animals lived beyond 24 days. The developmental larvae stages take the same time to happen (approximately 4 days).

This data suggests that C-terminal region of DLIC^{DLI-1}, and more specifically the conserved helix, have a significant impact in the longevity of the animals.

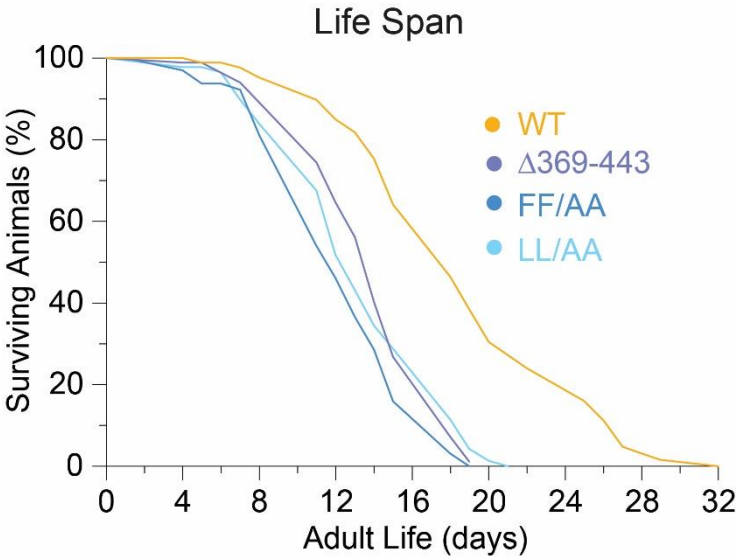

Figure 11 - Life span curves. Animals were synchronized by egg laying, collected as late L4 larvae (0 d) and followed every other day until they died. Wild-type (n=64), Δ369-443 (n=81), F392A/F393A (n=63), L396A/L397A (n=75).

The point mutations in helix1 of DLIC^{DLI-1} of worms impair locomotion.

Disruption of dynein function could lead to difficulties in motor neuron function and a decrease in the motility of the animals. *C. elegans* motility has been used as a read-out for motor neuron function. In order to assess if the *dli-1* mutations have a similar impact to null forms of *dli-1* and affect the motility of the animals we have done a liquid trashing assay. This assay consists in measuring the frequency of movement of the animal in liquid medium.

Homozygous AD1 *dli-1* mutants show striking defects in locomotion: wild-type animals, 1.50±0.02Hz, Δ369-443 animals 0.50±0.03Hz, F392/F393 animals 0.46±0.04Hz, L396A/L397A animals 0.50±0.0Hz.

These results show that the homozygous *dli-1* mutants move approximately 3-fold less than the wild-type clearly suggesting problems in motor neuron functions.

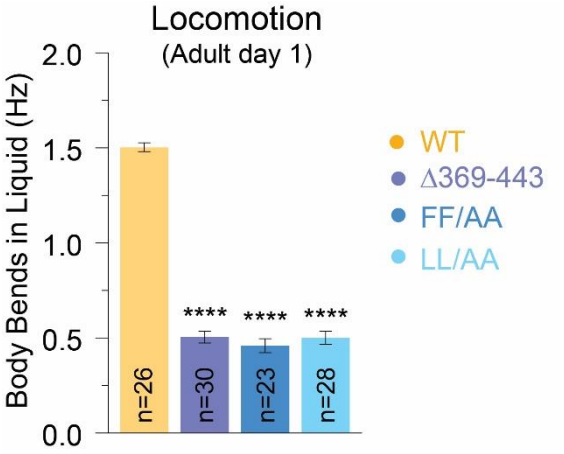

Figure 12 – Locomotion of *C. elegans* in liquid medium. Animal bends per second (Hz) in liquid medium were counted. Wild-type (n=26), Δ369-443 (n=30), F392/F393 (n=23), L396A/L397A (n=28). Graph shows mean ± SEM for *n* number of animals from two independent experiments. **** P<0.0001 for mutant vs. WT.

The point mutations in helix1 of DLIC^{DLI-1} lead to early endosomes and synaptic vesicles mis-accumulations in neurons.

Dynein-activity is essential for the normal functioning of retrograde axonal transport. In order to understand how affected is dynein motor complex functions when we mutate DLIC^{DLI-1} C-terminal region, we study the distribution of cargo in the axons of mechanosensory neurons of *C. elegans*. In wild-type neurons, the anterograde transport driven by kinesin transport cargos to the axonal terminal, and a balanced retrograde transport driven by dynein transport them towards the cell body. Interference with this balance, caused by dynein function disruption, should lead to a mis-accumulation of cargos at the axon terminals.

In order to allow the co-localization of neuronal processes and different known dynein-cargos, strains expressing soluble GFP under *mec4*, and early endosomes labelled by mKate2::RAB-5, expressed from the *mec7,* or synaptic vesicles labelled by SNB-1::mKate2, expressed from the *mec7* promotor, were constructed.

In this assay, we see all the three *dli-1* mutations cause mis-accumulation of early endosomes at the axonal tips of the anterior ALM and AVM neurons, in contrast to AD1 wild-type animals (Figure 13b). Additionally, observing only the architecture of the axons, the AD1-homozygous *dli-1* mutants show a beaded appearance, suggesting neurodegeneration (Figure 13b and c).

Furthermore, considering the described previous studies that identified mis-accumulation of synaptic vesicles in other *dli-1* mutants, we went on to study the distribution of synaptic vesicles in one of our three constructed mutants (dli-1 LL/AA).

Coincidently, we also identify mis-accumulation of this cargo at the tip of the anterior ALM and AVM neurons (Figure 13).

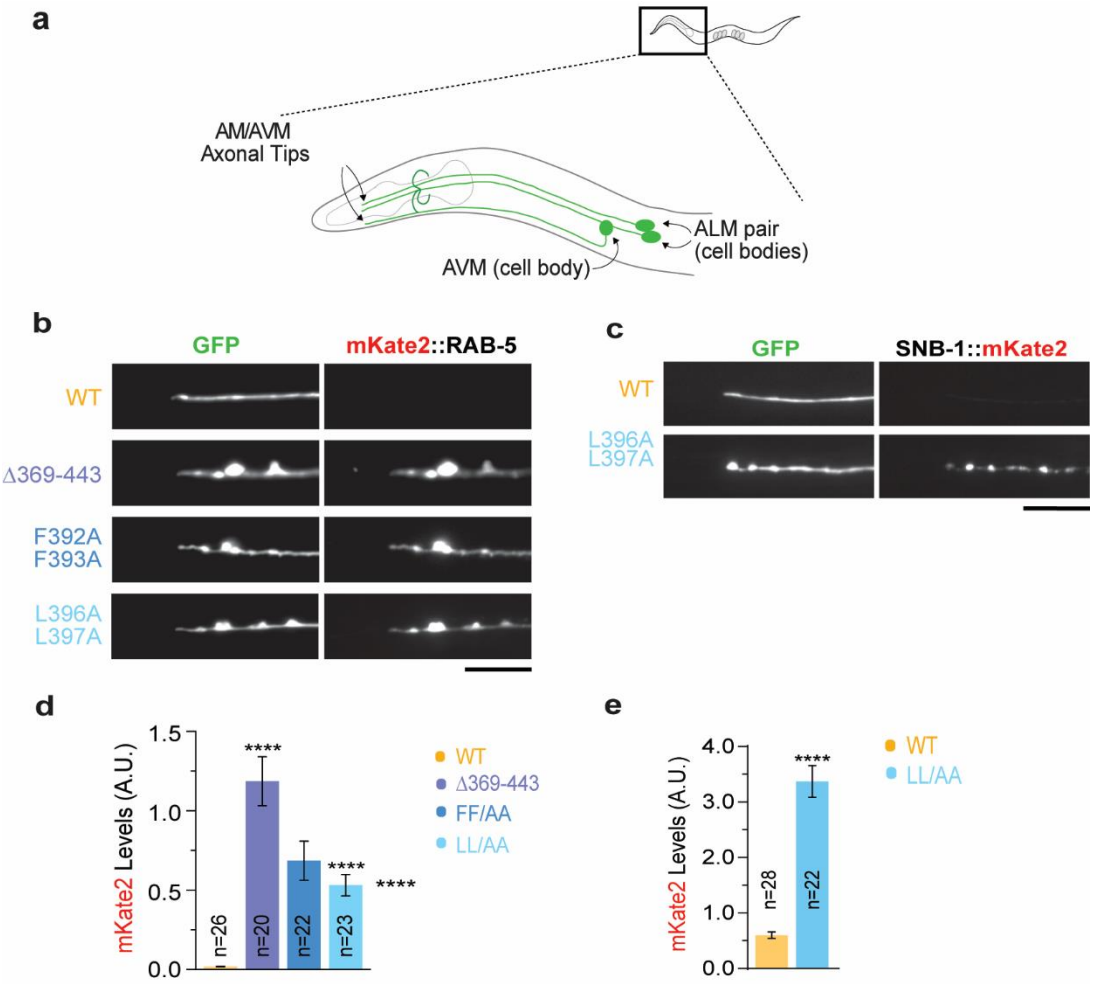

Figure 13 - Fluorescent images of axonal tips and quantifications. In the axonal tips of AVM/ALM mechanossensory neurons of AD1 animals (a), *dli-1* mutants have mis-accumulation of early endosomes (b, d) and synaptic vesicles (c, e). Scale bar: 10µm. Graph shows mean ± SEM for *n* number of animals from two independent experiments. **** P<0.0001 for mutant vs. WT

The mitochondrial axonal density in the mechanosensory neurons is modified by mutating DLIC^{DLI-1}.

The axonal transport of mitochondria by dynein happens in different conditions comparing to other organelles and cargos. Mitochondria are typically larger cargos, that can undergo fusion and fission, that frequently change direction of persistently dock for long periods. Taking this in consideration, we choose to study mitochondria (labelled by TOMM-20(1-54)::mKate2, expressed from *mec7* promotor) distribution along all axon.

Mutating DLIC^{DLI-1} helix1 does not change the overall mitochondria distribution along the axon. We see no significant differences between wild-type and L396A/L397A mutant in the percentage of TOMM-20 particles (mitochondria or mitochondria agglomerates), in the different sub regions of the axon (Figure 14). Curiously, counting the number of TOMM-20 particles along the axon, we saw an increase of 1.5 fold in the number of particles in the LL/AA mutant (Figure 14c). Moreover, in the L396A/L397A mutant, we saw a higher number of smaller particles, suggesting that we may have an increase in the mitochondria fission events (Figure 14b).

Additionally, since we were imaging the whole neuron in order to study the mitochondria distribution along the axon, we measured the length of the ALM neurons. We could see no difference in the length of the ALM neurons, between the wild-type and the L396A/L397A mutant animals (Figure 14).

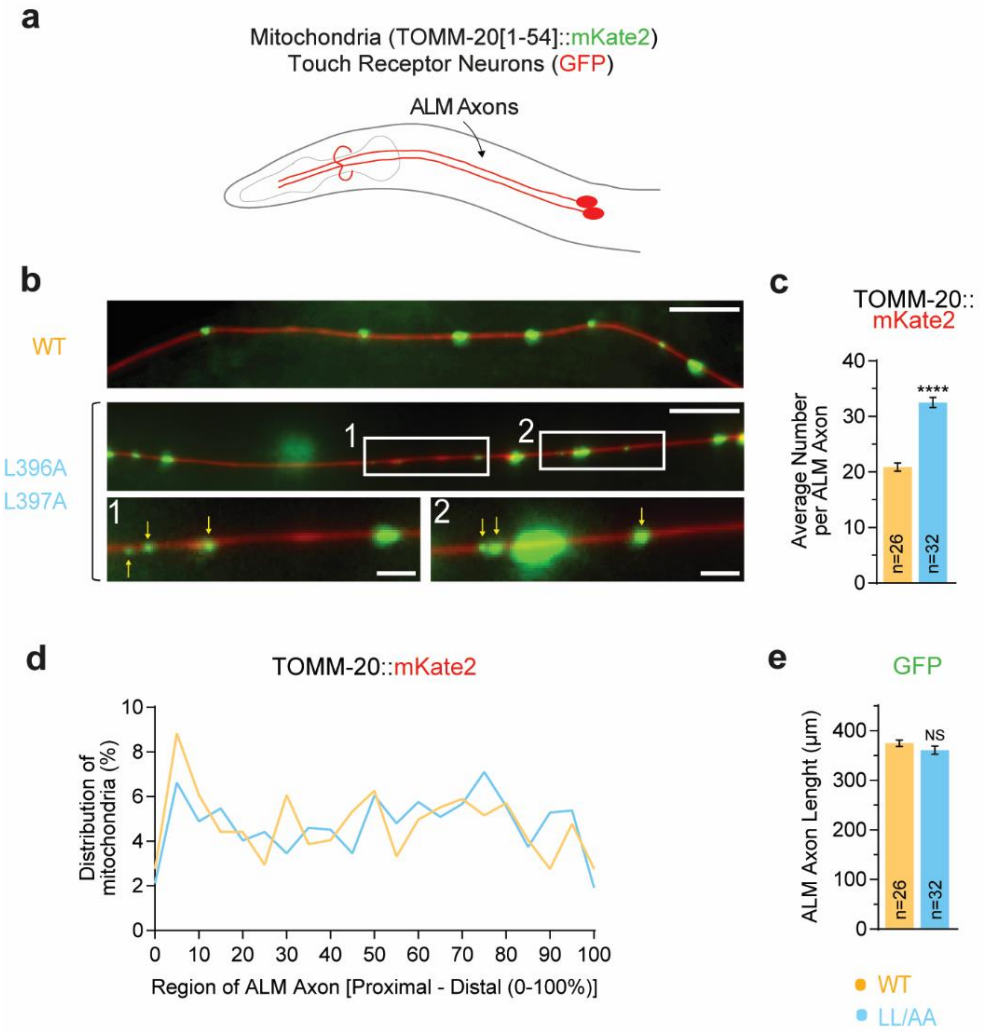

Figure 14 - Fluorescent images of the mitochondrial distribution in ALM axons and quantifications. In axon of mechanosensory ALM neuron in AD1 animals (a), *dli-1* mutant have an increase in the number of TOMM-20 particles along the ALM axon (b, c). No difference was observed in the overall mitochondrial distribution along the axon (d), and in the neuron length (e). Scale bar: 10 µm; Graph shows mean ± SEM for *n* number of animals from two independent experiments. **** P<0.0001 for mutant vs. WT; NS P>0.0001 for mutant vs. WT.

V. DISCUSSION AND CONCLUSION

Several neurodegenerative and neurodevelopmental diseases are associated with defects in axonal transport (Maday et al., 2014). Dynein is a well-known motor protein responsible for the retrograde microtubule-based transport, essential for normal trafficking in neurons. In order to perform its vast array of functions, dynein must be highly regulated. Currently, it is known that dynein must bind to dynactin and an adaptor protein to be highly processive.

Several adaptors were already described, and most of them were shown to bind to the C-terminal region of DLIC, an essential subunit. Some of these adaptors (Hook1/3, Spindly, BICD2, RFIP3) were shown to participate in the assembly and activation of the dynein motor complex (McKenney et al., 2014) and to depend on a conserved helix1 of DLIC C-terminal region to do so (Lee et al., 2018; unpublished results from our lab). These proteins and several others described as potential adaptors, appear to be important for the establishing of molecular bridges that link dynein to the cargo. Still, the *in vivo* significance of the $DLIC^{helix1}$ interaction with the adaptor proteins remains poorly described.

To study the function of the DLIC C-terminal region *in vivo*, we used CRISPR-Cas9 mediated genome editing to introduce three different mutations into the *C. elegans* DLIC homolog *dli-1* that were previously shown to disrupt the binding of DLIC to adaptors (unpublished results from our lab; Lee et al., 2018).

Considering that DLIC is essential for the DHC stability (King et al., 2002; Trokter et al., 2012), we wanted to assess if DHC-1 levels could be drastically decreased by the introduction of the mutations. In order to analyze that hypothesis, we have done an immunoblot to DHC-1 in protein extracts of the three mutants. The results have shown that the DHC-1 levels are not decreased. In fact, the immunoblot has shown that in the three constructed mutants we have a slight increase in DHC-1 expression that may constitute a cellular mechanism of compensation.

The deletion of the C-terminal region, and the two-aminoacid substitutions in four conserved residues of the helix1 (phenylalanine392 and phenylalanine393, and leucine396 and leucine397) led to a severe phenotype, causing sterility in the homozygous animals. Using differential interference contrast microscopy in the three homozygous *dli-1* mutants showed with detail the presence of severe morphological and developmental defects, similar between the three mutants.

These animals have slightly dumpy bodies, disorganized gonads incapable to produce embryos, and protruding vulvas. This phenotype may arise from the failure of cell division in numerous of postembryonic cell lineages in the described mutants. The

failure of cell division during the tissue-specification process led to the formation of a disorganized and malfunctioning gonad. A previous study characterizing strong loss-of-function mutations on *dli-1* showed that the observed cell division failure affects several postembryonic lineages such as vulva precursor cells and their descendants, hypodermal cells, and cells of the gonad (germline and somatic) (Yoder and Han, 2001).

DLIC is now known to be important for binding of several activators that properly activate the motor, after the assembly of the motor complex. Several studies describe that the depletion of the two isoforms of DLIC in human cells result in centrosome mispositioning (Raaijmakers et al., 2013). In *C. elegans* embryos, DLI-1^{DLIC} showed to be required for discrete aspects of mitosis, more specifically in pronuclear migration, centrosome separation and association to the male pronucleus (Yoder and Han, 2001). These discrete defects were only observed in the mitosis of *C. elegans* embryos. The context of a single-cell model may not be sufficient to reveal the significance of this subunit, and more specifically the helix1 of the C-terminal region of DLIC. These results have shown that the helix1 of DLIC^{DLI-1} is essential for the development and fertility of *C. elegans*.

The morphological defects described are perceptible only after the L4-stage. The failure of postembryonic mitotic cell divisions does not compromise animal viability even though they result the sterility. The early larval lineages are not affected by the introduced mutations, and only after the total depletion of the maternal wild-type protein with the beginning of gene expression in *C. elegans* embryos, we start seeing morphological and developmental defects.

In order to fully understand how disrupting DLIC^{DLI-1} helix1 affect dynein motor complex functions, we went on to study dynein in cargo axonal transport. Several years ago, it became clear that, in *Drosophila*, mutations on dynein components leads to defects in transport of synaptic vesicles, and endosomal cargo becomes blocked in axons (Martin et al., 1999). Moreover, it is known that a wide diversity of cargos are transported by dynein in axons, and that DLIC subunit may have an essential role in this transport by mediate the binding to the different adaptors. Koushika *et al.* also described that DLI-1 has an important role in axonal retrograde transport of *C. elegans* (Koushika, 2004).

Aiming to understand how the dynein motor is affected when we mutate DLI-1 C-terminal region, we studied the distribution of early endosomes, synaptic vesicles, and mitochondria in neurons. Early endosomes are known dynein-cargos that move in axon either in retrograde or anterograde direction. In order to localize them, we fluorescently labelled Rab5, a Ras-related protein known to be associated in the maturation of early endosomes (Flores-Rodriguez et al., 2011). Synaptic vesicles are neuronal organelles

transported by dynein towards the synaptic compartment in neurons. Similar to Rab5, we used synaptobrevin, which is associated to synaptic vesicles, as a marker for these organelles in several studies (Baumert et al., 1989; Koushika et al., 2004). The imaging of early endosomes or synaptic vesicles in neurons made possible to analyse the distribution of these cargos in the tip of the axon in the wild-type and in the *dli-1* mutant animals. In wild-type animals, early endosomes and synaptic vesicles are known to initiate its movement at the tip of the axons and be transported by dynein towards the cell body.

Concerning early endosome distribution, we saw that all mutants mis-accumulate early endosomes at the axon tips, suggesting problems in the initiation of the retrograde transport. In order to confirm that this mis-accumulation arise from problems in retrograde transport, more experiments were conducted in our lab. We studied the kinetic of early endosomes in the axon by imaging with high temporal resolution in an axonal segment close to the cell body. In this quantitative analysis, we observed that the three *dli-1* mutants have similar cargo's motility behaviour (unpublished results from our lab). Since no difference was found between the dli-1 Δ369-443 and the dli-1 L396A/L397A and dli-1 F392A/F393A mutants, it appears that the most important region for the dynein-interaction with the adaptors is the conserved helix1. These results go in accordance with the described biochemical results from our lab, and confirm the relevance of the interaction dynein-adaptor in dynein-cargo transport functions.

Following the previous results from Koushika et al. (Koushika, 2004), we addressed distribution of synaptic vesicles at the tip of the axons in our L396A/L387A mutant. In this assay, we also identified mis-accumulation of synaptic vesicles at the tip of the anterior ALM and AVM neurons compared to what was previous described for *dli-1* null mutant.

Even though all mutants have the mis-accumulation of dynein-cargos at the axonal terminals, one curious result observed was that, regarding early endosomes, the *dli-1* Δ369-443 led to a slightly more obvious mis-accumulation of early endosomes than the point mutants do. We think that this result highlights the importance of the integrity of the $DLIC^{DLI-1}$ C-terminal region. In one recent study, the conserved helix1 of $DLIC^{DLI-1}$ was show being the most important region for the interaction of DLIC with the adaptors (Lee et al., 2018) which goes in accordance to our biochemical findings. Although this interaction is essential, it appears that additional contacts with the other residues of the C-terminal region may be important for these interactions. These results show that the helix1 of the C-terminal region of $DLIC^{DLI-1}$ is important for the transport of early endosomes towards the cell body; however, additional residues of the remaining C-terminal region may be needed to a more efficient interaction.

Overall, this analysis revealed that all the three *dli-1* mutants have strongly impaired retrograde axonal transport of early endosomes and synaptic vesicles, consistent with compromised dynein function.

Aiming to understand how this compromised dynein function could influence the transport of larger cargos; we studied the distribution of mitochondria along the axon. To study mitochondria distribution, we fluorescently labelled TOMM-20, a mitochondrial import receptor. Mitochondria have a different motility behaviour in comparison to other cargos: this organelle can undergo fusion and fission, change its direction several times, and may pause and dock for several time in one place with higher metabolic demands.

Our results show that there are no differences between mutant and wild-type in mitochondria distribution along the axon. This observation on overall distribution does not exclude that mitochondrial motility is altered in our mutants. However, in the *dli-1* mutant we saw an increase in the density of mitochondria particles with smaller sizes compared to the ones observed in the wild-type animals. Curiously, a different result was described in a recent paper that studied the mitochondria distribution in *null* mutants of DLI-1, and saw a decrease in the mitochondrial density (Sure et al., 2018). Taking in consideration that dynein-transport should be impaired by mutating $DLIC^{DLI-1}$, we should see a decrease in the mitochondrial distribution since dynein will not be able to transport mitochondria towards the cell body. However, several studies describe that neurodegenerative diseases are associated with an imbalance in the mitochondria fission/fusion events (Knott et al., 2008). In addition, it was also observed that AD1-homozygous *dli-1* mutants have an axonal architecture with a beaded appearance, an established hallmark of degeneration.

Other phenotypes observed in our mutants appear to confirm that the disruption of dynein transport function in axons directly affect neuron survival and functions, leading to neurodegeneration. Our additional assays that evaluated the motility and life span of the mutants appear to agree with this hypothesis.

Although the mutant animals developed in the same period than the wild-type animals, at the beginning of adult-stage the severe morphological defects already described and higher lipofuscin levels along the animal body start to appear (data not shown). Accelerated aging and shorter life expectancy is associated with decrepit-looking (Herndon et al., 2002), and higher lipofuscin loads (Pincus and Slack, 2010) in the animals. Our longevity assay confirmed that the three *dli-1* mutants have significant shorten life span. Longevity is known to be influenced by several genetic and stochastic factors. Even in a synchronized isogenic *C. elegans* population grown in the same conditions, worms age differently and die at different time points (Herndon et al., 2002). Neurons have been shown to regulate animal longevity, since defects in neuronal

signalling may intensify physiological aging (Wolkow et al., 2000; Bishop and Guarente, 2007).

Measuring *C. elegans*' locomotion also showed that, as predicted, the helix1 of DLI-1 has an essential role in the motor neuron function. The impairment in locomotion observed in the three DLI-1 mutants suggests that the neuronal function is defective in our mutants. The neuron functions and survival depend on the balance between retrograde and anterograde transport. The degradative traffic and survival signalling both depend on the well functioning of the retrograde transport.

After characterizing the morphology, life span and motility of the three constructed mutants, we believe that mutating DLI-1 C-terminal region in *C. elegans* disrupt dynein-mediated cargo transport in neurons. DLI-1 C-terminal region, more specifically the conserved helix1, seems to be important for the binding to several adaptors and to establish molecular bridges that mediate the binding to several cargos. Our results also add that not all cargos may be affected in the same way by the absence of DLI-1 C-terminal region or by the disruption of the conserved helix1. Additional contacts are possibly compensating, being sufficient for the cargo's transport.

In summary, mutating DLI-1 helix1 in *C. elegans*, we saw what appears to be an enhancement of the neurodegeneration process observed by shorten life span, impairment in the locomotion, neurons with beaded appearance and finally, an apparent increase in mitochondria fission events.

The disruption of the interaction between DLIC with cargo adaptors caused by the mutations on helix1 may enhance neurodegeneration, by severely affecting dynein transport functions in neurons.

REFERENCES

Alloatti, M., Bruno, L., Falzone, T.L., 2018. Methods for Quantitative Analysis of Axonal Cargo Transport, in: Skaper, S.D. (Ed.), Neurotrophic Factors: Methods and Protocols, Methods in Molecular Biology. Springer. doi:10.1007/978-1-4939-7571-6_16

Arimoto, M., Koushika, S.P., Choudhary, B.C., Li, C., Matsumoto, K., Hisamoto, N., 2011. The Caenorhabditis elegans JIP3 Protein UNC-16 Functions As an Adaptor to Link Kinesin-1 with Cytoplasmic Dynein 31, 2216–2224. doi:10.1523/JNEUROSCI.2653-10.2011

Arribere, J.A., Bell, R.T., Fu, B.X.H., Artiles, K.L., Hartman, P.S., Fire, A.Z., 2014. Efficient Marker-Free Recovery of Custom Genetic Modi fi cations with CRISPR / Cas9. Genetics 198, 837–846. doi:10.1534/genetics.114.169730

Ayloo, S., Lazarus, J.E., Dodda, A., Tokito, M., Ostap, E.M., Holzbaur, E.L.F., 2014. Dynactin functions as both a dynamic tether and brake during dynein-driven motility. Nat. Commun. 5, 4807. doi:10.1038/ncomms5807

Baumert, M., Maycox, P.R., Navone, F., De Camilli, P., Jahn, R., 1989. Synaptobrevin: an integral membrane protein of 18,000 daltons present in small synaptic vesicles of rat brain. EMBO J. 8, 379–84.

Bielska, E., Schuster, M., Roger, Y., Berepiki, A., Soanes, D.M., Talbot, N.J., Steinberg, G., 2014. Hook is an adapter that coordinates kinesin-3 and dynein cargo attachment on early endosomes. J. Cell Biol.

Bishop, N.A., Guarente, L., 2007. Two neurons mediate diet-restriction-induced longevity in C. elegans. Nature 447, 545–549. doi:10.1038/nature05904

Cantalupo, G., Alifano, P., Roberti, V., Bruni, C.B., Bucci, C., 2001. Rab-interacting lysosomal protein (RILP): the Rab7 effector required for transport to lysosomes 20, 683–693.

Caviston, J.P., Ross, J.L., Antony, S.M., Tokito, M., Holzbaur, E.L.F., 2007. Huntingtin facilitates dynein/dynactin-mediated vesicle transport. Proc. Natl. Acad. Sci. 104, 10045–10050. doi:10.1073/pnas.0610628104

Chalfie, M., Thomson, J.N., 1979. Organization of Neuronal Microtubules in the Nematode Caenorhabditis elegans. J. Cell Biol. doi:10.1083/jcb.82.1.278

Chen, C., Fenk, L.A., Bono, M. De, 2013. Efficient genome editing in Caenorhabditis elegans by CRISPR-targeted homologous recombination 41. doi:10.1093/nar/gkt805

Chevalier-larsen, E., Holzbaur, E.L.F., 2006. Axonal transport and neurodegenerative disease 1762, 1094–1108. doi:10.1016/j.bbadis.2006.04.002

Cianfrocco, M.A., Desantis, M.E., Leschziner, A.E., Reck-peterson, S.L., 2015. Mechanism and Regulation of Cytoplasmic Dynein 1–26. doi:10.1146/annurev-cellbio-100814-125438

Course, M.M., Wang, X., 2016. Transporting mitochondria in neurons [version 1 ; referees : 2 approved] Referee Status : 5, 1–10. doi:10.12688/f1000research.7864.1

Dickinson, D.J., Goldstein, B., 2016. CRISPR-Based Methods for Caenorhabditis elegans Genome Engineering. Genetics 202, 885–901. doi:10.1534/genetics.115.182162

Dickinson, D.J., Ward, J.D., Reiner, D.J., Goldstein, B., 2013. Engineering the Caenorhabditis elegans genome using Cas9-triggered homologous recombination. Nat. Methods 1–9. doi:10.1038/nmeth.2641

Dixit, R., Ross, J.L., Goldman, Y.E., Holzbaur, E.L.F., 2008. Differential Regulation of Dynein and Kinesin Motor Proteins by Tau. Science (80-.). 319, 1086–1089. doi:10.1126/science.1152993.Differential

Echeverri, C.J., Paschal, B.M., Vaughan, K.T., Vauee, R.B., 1996. Molecular Characterization of the 50-kD Subunit of Dynactin Reveals Function for the Complex in Chromosome Alignment and Spindle Organization during Mitosis 132.

Flores-Rodriguez, N., Rogers, S.S., Kenwright, D.A., Waigh, T.A., Woodman, P.G., Allan, V.J., 2011. Roles of dynein and dynactin in early endosome dynamics revealed using automated tracking and global analysis. PLoS One 6. doi:10.1371/journal.pone.0024479

Gama, J.B., Pereira, C., Simões, P.A., Celestino, R., Reis, R.M., Barbosa, D.J., Pires, H.R., Carvalho, C., Amorim, J., Carvalho, A.X., Cheerambathur, D.K., 2017. Molecular mechanism of dynein recruitment to kinetochores by the Rod – Zw10 – Zwilch complex and Spindly.

Genome Sequence of the Nematode C. elegans: A Platform for Investigating Biology, 1998.

Gill, S.R., Schroer, T.A., Szilak, I., Steuer, E.R., Sheetz, M.P., Cleveland, D.W., 1991. Dynactin, a conserved, ubiquitously expressed component of an activator of vesicle motility mediated by cytoplasmic dynein. J. Cell Biol. 115, 1639–50.

Guo, X., Farías, G.G., Mattera, R., Bonifacino, J.S., 2016. Rab5 and its effector FHF contribute to neuronal polarity through dynein-dependent retrieval of somatodendritic proteins from the axon 5318–5327. doi:10.1073/pnas.1601844113

Ham, H., Huynh, W., Schoon, R.A., Vale, R.D., Billadeau, D.D., 2015. HkRP3 Is a Microtubule-Binding Protein Regulating Lytic Granule Clustering and NK Cell Killing. J. Immunol. 194, 3984–3996. doi:10.4049/jimmunol.1402897

Herndon, L.A., Schmeissner, P.J., Dudaronek, J.M., Brown, P.A., Listner, K.M., Sakano, Y., Paupard, M.C., Hall, D.H., Driscoll, M., 2002. Stochastic and genetic factors influence tissue-specific decline in ageing C. elegans. Nature 419, 808–814. doi:10.1038/nature01135

Hirokawa, N., Niwa, S., Tanaka, Y., 2010. Review Molecular Motors in Neurons : Transport Mechanisms and Roles in Brain Function , Development , and Disease. Neuron 68, 610–638. doi:10.1016/j.neuron.2010.09.039

Holzbaur, E.L.F., Hammarback, J.A., Paschal, B.M., Kravit, N.G., Pfister, K.K., Vallee, R.B., 1991. Homology of a 150K cytoplasmic dynein-associated polypeptide with the Drosophila gene Glued. Nature 351, 579–583. doi:10.1038/351579a0

Hoogenraad, C.C., Akhmanova, A., 2016. Bicaudal D Family of Motor Adaptors : Linking Dynein Motility to Cargo Binding. Trends Cell Biol. 1–14. doi:10.1016/j.tcb.2016.01.001

Hoogenraad, C.C., Wulf, P., Schiefermeier, N., Stepanova, T., Galjart, N., Small, J.V., Grosveld, F., Zeeuw, C.I. De, Akhmanova, A., 2003. Bicaudal D induces selective dynein-mediated microtubule minus end-directed transport 22.

Horgan, C.P., Hanscom, S.R., Jolly, R.S., Futter, C.E., Mccaffrey, M.W., 2010. Rab11-FIP3 links the Rab11 GTPase and cytoplasmic dynein to mediate transport to the endosomal- recycling compartment. doi:10.1242/jcs.052670

Hueschen, C.L., Kenny, S.J., Xu, K., Dumont, S., 2017. NuMA recruits dynein activity to microtubule minus-ends at mitosis. Elife 6. doi:10.7554/eLife.29328

Hughes, S.M., Vaughan, K.T., Herskovits, J.S., Vallee, R.B., 1995. Molecular analysis of a cytoplasmic dynein light intermediate chain reveals homology to a family of ATPases 24, 17–24.

Jordens, I., Fernandez-Borja, M., Marsman, M., Dusseljee, S., Janssen, L., Calafat, J., Janssen, H., Wubbolts, R., Neefjes, J., 2001. The Rab7 effector protein RILP controls lysosomal transport by inducing the recruitment of dynein-dynactin motors. Curr. Biol. doi:10.1016/S0960-9822(01)00531-0

Kardon, J.R., Vale, R.D., 2009. Regulators of the cytoplasmic dynein motor. Nat. Rev. Mol. Cell Biol. 10, 854–865. doi:10.1038/nrm2804

King, S.J., Bonilla, M., Rodgers, M.E., Schroer, T.A., 2002. Subunit organization in cytoplasmic dynein subcomplexes 1239–1250. doi:10.1110/ps.2520102.large

Knott, A.B., Perkins, G., Schwarzenbacher, R., Bossy-Wetsel, E., 2008. Mitochondrial fragmentation in neurodegeneration. Nat. Rev. Neurosci. 9, 505–518. doi:10.1038/nrn2417.MITOCHONDRIAL

Koushika, S.P., 2004. Mutations in Caenorhabditis elegans Cytoplasmic Dynein Components Reveal Specificity of Neuronal Retrograde Cargo. J. Neurosci. doi:10.1523/JNEUROSCI.5039-03.2004

Koushika, S.P., Nonet, M.L., 2000. Sorting and transport in C . elegans : a model system with a sequenced genome. Curr. Opin. Cell Biol. 517–523.

Koushika, S.P., Schaefer, A.M., Vincent, R., Willis, J.H., Bowerman, B., Nonet, M.L., 2004. Mutations in Caenorhabditis elegans Cytoplasmic Dynein Components Reveal Specificity of Neuronal Retrograde Cargo 24, 3907–3916. doi:10.1523/JNEUROSCI.5039-03.2004

Lee, I., Olenick, M.A., Boczkowska, M., Franzini-armstrong, C., Holzbaur, E.L.F., Dominguez, R., 2018. A conserved interaction of the dynein light intermediate chain with dynein-dynactin effectors necessary for processivity. Nat. Commun. doi:10.1038/s41467-018-03412-8

Liu, J., 2017. Regulation of dynein-dynactin-driven vesicular transport 336–347. doi:10.1111/tra.12475

Maday, S., Twelvetrees, A.E., Moughamian, A.J., Holzbaur, E.L.F., 2014. Review Axonal Transport : Cargo-Specific Mechanisms of Motility and Regulation. Neuron 84, 292–309. doi:10.1016/j.neuron.2014.10.019

Martin Chalfie, 1990. The Differentiation of Touch Receptor Neurons in Cenorhabditis elegans: A case study of genetic and molcecular analysis. Am. Zool.

Martin, M., Iyadurai, S.J., Gassman, A., Gindhart, J.G., Hays, T.S., Saxton, W.M., 1999.

Cytoplasmic Dynein , the Dynactin Complex , and Kinesin Are Interdependent and Essential for Fast Axonal Transport 10, 3717–3728.

Matanis, T., Akhmanova, A., Wulf, P., Del Nery, E., Weide, T., Stepanova, T., Galjart, N., Grosveld, F., Goud, B., De Zeeuw, C.I., Barnekow, A., Hoogenraad, C.C., 2002. Bicaudal-D regulates COPI-independent Golgi-ER transport by recruiting the dynein-dynactin motor complex. Nat. Cell Biol. doi:10.1038/ncb891

Matanis, T., Akhmanova, A., Wulf, P., Nery, E. Del, Weide, T., Stepanova, T., Galjart, N., Grosveld, F., Goud, B., Zeeuw, C.I. De, Barnekow, A., Hoogenraad, C.C., 2003. Bicaudal-D regulates COPI-independent Golgi – ER transport by recruiting the dynein – dynactin motor complex 4. doi:10.1038/ncb891

McKenney, R.J., Huynh, W., Tanenbaum, M.E., Bhabha, G., Vale, R.D., 2014. Activation of cytoplasmic dynein motility by dynactin-cargo adapter complexes. Science (80-.). doi:10.1126/science.1254198

Mondal, S., Ahlawat, S., Rau, K., Venkataraman, V., Koushika, S.P., 2011. Imaging in vivo Neuronal Transport in Genetic Model Organisms Using Microfluidic Devices. Traffic 12, 372–385. doi:10.1111/j.1600-0854.2010.01157.x

Nair, A., Ramanarayanan, S., Ahlawat, S., Koushika, S., Joshi, N., Sivaprakasam, M., 2014. Axonal transport velocity estimation from kymographs based on curvilinear feature extraction and spline fitting, in: 2014 36th Annual International Conference of the IEEE Engineering in Medicine and Biology Society. IEEE, pp. 4240–4243. doi:10.1109/EMBC.2014.6944560

Nirschl, J.J., Ghiretti, A.E., Holzbaur, E.L.F., 2017. The impact of cytoskeletal organization on the local regulation of neuronal transport. Nat. Publ. Gr. 18, 585–597. doi:10.1038/nrn.2017.100

Paschal, B.M., Shpetner, H.S., Vallee, R.B., 1987. MAP 1C is a microtubule-activated ATPase which translocates microtubules in vitro and has dynein-like properties. J. Cell Biol. 105, 1273–82.

Pilling, A.D., Horiuchi, D., Lively, C.M., Saxton, W.M., 2006. Kinesin-1 and Dynein Are the Primary Motors for Fast Transport of Mitochondria in Drosophila Motor Axons □ 17, 2057–2068. doi:10.1091/mbc.E05

Pincus, Z., Slack, F.J., 2010. Developmental biomarkers of aging in C. elegans. Dev. Dyn. doi:10.1002/dvdy.22224

Presley, J.F., Cole, N.B., Schroer, T.A., 1997. ER-to-Golgi transport visualized in living cells 17123, 17119–17123.

Progida, C., Malerød, L., Stuffers, S., Brech, A., Bucci, C., Stenmark, H., 2007. RILP is required for the proper morphology and function of late endosomes 101. doi:10.1242/jcs.017301

Quintyne, N.J., Gill, S.R., Eckley, D.M., Crego, C.L., Compton, D.A., Schroer, T.A., 1999. Dynactin Is Required for Microtubule Anchoring at Centrosomes 147, 321–334.

Raaijmakers, J.A., Tanenbaum, M.E., Medema, R.H., 2013. Systematic dissection of dynein regulators in mitosis. J. Cell Biol. 201, 201–215. doi:10.1083/jcb.201208098

Raj, F., Amrit, G., Ratnappan, R., Keith, S.A., Ghazi, A., 2014. The C . elegans lifespan assay toolkit. Methods 68, 465–475. doi:10.1016/j.ymeth.2014.04.002

Ran, F.A., Hsu, P.D., Wright, J., Agarwala, V., Scott, D.A., Zhang, F., 2013. Genome engineering using the CRISPR-Cas9 system 8, 2281–2308. doi:10.1038/nprot.2013.143

Rao, A.N., Baas, P.W., 2017. Polarity Sorting of Microtubules in the Axon. Trends Neurosci. xx, 1–12. doi:10.1016/j.tins.2017.11.002

Reck-Peterson, S.L., Redwine, W.B., Vale, R.D., Carter, A.P., 2018. The cytoplasmic dynein transport machinery and its many cargoes. Nat. Rev. Mol. Cell Biol. doi:10.1038/s41580-018-0004-3

Redwine, W.B., Desantis, M.E., Hollyer, I., Htet, Z.M., Tran, P.T., Swanson, S.K., Florens, L., Washburn, M.P., Reck-peterson, S.L., 2017. The human cytoplasmic dynein interactome reveals novel activators of motility 1–27. doi:10.7554/eLife.28257

Roberts, A.J., 2018. Emerging mechanisms of dynein transport in the cytoplasm versus the cilium. Biochem. Soc. Trans. 0, 1–16. doi:10.1042/BST20170568

Roberts, A.J., Kon, T., Knight, P.J., Sutoh, K., Burgess, S.A., 2013. Functions and mechanics of dynein motor proteins. Nat. Publ. Gr. doi:10.1038/nrm3667

Rok, K., Yup, S., 2016. CRISPR technologies for bacterial systems : Current achievements and future directions. Biotechnol. Adv. doi:10.1016/j.biotechadv.2016.08.002

Schlager, M. a, Hoang, H.T., Urnavicius, L., Bullock, S.L., Carter, A.P., 2014. In vitro reconstitution of a highly processive recombinant human dynein complex. EMBO J. 33, 1–14. doi:10.15252/embj.201488792

Schlager, M.A., Serra-marques, A., Grigoriev, I., Gumy, L.F., Esteves, M., Wulf, P.S., Akhmanova, A., Hoogenraad, C.C., 2014. Report Bicaudal D Family Adaptor Proteins Control the Velocity of Dynein-Based Movements. CellReports 8, 1248–1256. doi:10.1016/j.celrep.2014.07.052

Schroeder, C.M., Ostrem, J.M.L., Hertz, N.T., Vale, R.D., 2014. A Ras-like domain in the light intermediate chain bridges the dynein motor to a cargo-binding region 1–22. doi:10.7554/eLife.03351

Schroeder, C.M., Vale, R.D., 2016. Assembly and activation of dynein – dynactin by the cargo adaptor protein Hook3 214. doi:10.1083/jcb.201604002

Sivaram, M.V.S., Wadzinski, L., Redick, S.D., Manna, T., Doxsey, S.J., 2009. Dynein light intermediate chain 1 is required for progress through the spindle assembly checkpoint 28, 1–13. doi:10.1038/emboj.2009.38

Sood, P., Murthy, K., Kumar, V., Nonet, M.L., Menon, G.I., Koushika, S.P., 2018. Cargo crowding at actin-rich regions along axons causes local traffic jams. Traffic 19, 166–181. doi:10.1111/tra.12544

Splinter, D., Razafsky, D.S., Schlager, M., Serra-Marques, A., Grigoriev, I., Demmers, J., Keijzer, N., Jiang, K., Poser, I., Hyman., Hoogenraad, C.C., King, S.J., Akhmanova, A., 2012. BICD2, dynactin, and LIS1 cooperate in regulating dynein recruitment to cellular structures. Mol. Biol. Cell 23, 4226–4241. doi:10.1091/mbc.E12-03-0210

Stepanova, T., Slemmer, J., Hoogenraad, C.C., Lansbergen, G., Dortland, B., Zeeuw, C.I. De, Grosveld, F., Cappellen, G. Van, Akhmanova, A., Galjart, N., 2003.

Visualization of Microtubule Growth in Cultured Neurons via the Use of EB3-GFP (End-Binding Protein 3-Green Fluorescent Protein) 23, 2655–2664.

Sure, G.R., Chatterjee, A., Mishra, N., Sabharwal, V., 2018. UNC-16 / JIP3 and UNC-76 / FEZ1 limit the density of mitochondria in C . elegans neurons by maintaining the balance of anterograde and retrograde mitochondrial transport. Sci. Rep. 1–12. doi:10.1038/s41598-018-27211-9

Sutphin, G.L., Kaeberlein, M., 2009. Measuring Caenorhabditis elegans Life Span on Solid Media Part 3 : Score animals for life span 1–7. doi:10.3791/1152

Szebenyi, G., Hall, B., Yu, R., Hashim, A.I., Krämer, H., 2007. Hook2 Localizes to the Centrosome, Binds Directly to Centriolin/CEP110 and Contributes to Centrosomal Function. Traffic 8, 32–46. doi:10.1111/j.1600-0854.2006.00511.x

Tan, S.C., Scherer, J., Vallee, R.B., 2011. Recruitment of dynein to late endosomes and lysosomes through light intermediate chains 22. doi:10.1091/mbc.E10-02-0129

Terenzio, M., Golding, M., Russell, M.R.G., Wicher, K.B., Rosewell, I., Spencer-dene, B., Ish-horowicz, D., Schiavo, G., 2014. Bicaudal-D 1 regulates the intracellular sorting and signalling of neurotrophin receptors 33, 1582–1598.

Trokter, M., Mücke, N., Surrey, T., 2012. Reconstitution of the human cytoplasmic dynein complex 109, 20895–20900. doi:10.1073/pnas.1210573110

Urnavicius, L., Lau, C.K., Elshenawy, M.M., Morales-rios, E., Motz, C., 2017. Cryo-EM shows how dynactin recruits two dyneins for faster movement.

Urnavicius, L., Zhang, K., Diamant, A.G., Motz, C., Schlager, M.A., Yu, M., Patel, N.A., Robinson, C. V, Carter, A.P., 2015. The structure of the dynactin complex and its interaction with dynein. Science (80-.). 347, 1441–1446. doi:10.1126/science.aaa4080

van Spronsen, M., Mikhaylova, M., Lipka, J., Schlager, M.A., van den Heuvel, D.J., Kuijpers, M., Wulf, P.S., Keijzer, N., Demmers, J., Kapitein, L.C., Jaarsma, D., Gerritsen, H.C., Akhmanova, A., Hoogenraad, C.C., 2013. TRAK/Milton Motor-Adaptor Proteins Steer Mitochondrial Trafficking to Axons and Dendrites. Neuron 77, 485–502. doi:10.1016/j.neuron.2012.11.027

Wang, Y., Huynh, W., Skokan, T.D., Vale, R.D., 2018. A new calcium-activated dynein adaptor protein , CRACR2a , regulates clathrin- independent endocytic traffic in T cells.

White, J.G., Southgate, E., Thomson, J.N., Brenner, S., 1986. The structure of the nervous system of the nematode Caenorhabditis elegans. Philos. Trans. R. Soc. Lond. B. Biol. Sci. 314, 1–340. doi:10.1098/RSTB.1986.0056

Wolkow, C.A., Kimura, K.D., Lee, M.S., Ruvkun, G., 2000. Regulation of C. elegans life-span by insulinlike signaling in the nervous system. Science 290, 147–50. doi:10.1126/SCIENCE.290.5489.147

Xu, S., 2015. The Application of CRISPR-Cas9 Genome Editing in Caenorhabditis elegans. J. Genet. Genomics 42, 413–421. doi:10.1016/j.jgg.2015.06.005

Yoder, J.H., Han, M., 2001. Required for Discrete Aspects of Mitosis in Caenorhabditis elegans 12, 2921–2933.

Zhang, K., Foster, H.E., Rondelet, A., Lacey, S.E., Bahi-buisson, N., Bird, A.W., Carter,

A.P., Zhang, K., Foster, H.E., Rondelet, A., Lacey, S.E., Bahi-buisson, N., Bird, A.W., Carter, A.P., 2017. Cryo-EM Reveals How Human Cytoplasmic Dynein Is Article Cryo-EM Reveals How Human Cytoplasmic Dynein Is Auto-inhibited and Activated. Cell 169, 1303–1314.e18. doi:10.1016/j.cell.2017.05.025

VI. SUPPLEMENTARY DATA

Table S1 - Dynein adaptor proteins, putative domain of binding to DLIC [proteins already proved to bind DLIC are labelled with an asterisk, and domains proved to bind DLIC are labelled with two asterisk (McKenney et al., 2014; Schroeder et al., 2014; Schroeder and Vale, 2016; Gama et al., 2017; Redwine et al., 2017; Wang et al., 2018)] and associated cargo. The proved activating adaptors are in blue, the candidate activating adaptors are in green, and other proteins that may be associated are in yellow.

ADAPTOR PROTEIN	DOMAIN OF PUTATIVE BINDING TO DLIC	CARGO	REFERENCES
Hook1 **Hook3***	Hook domain**	RAB5 early endosomes	(McKenney et al., 2014; Guo et al., 2016; Schroeder and Vale, 2016; Lee et al., 2018)
BICD2* **BICDL1**	CC1-box domain**	Golgi vesicles, nuclear pore complexes, RAB6 vesicles	(Hoogenraad et al., 2003; McKenney et al., 2014; M. a Schlager et al., 2014; Urnavicius et al., 2017)
NIN* **NINL**	EF-hand pair	Unknown	(Redwine et al., 2017)
RFIP3*	EF-hand pair	Recycling endosomes	(Horgan et al., 2010; McKenney et al., 2014)
Spindly*	CC1-box domain**	Kinetochores	(McKenney et al., 2014; Gama et al., 2017)
CRACR2a	EF-hand pair	Distinct endosomal populations	(Wang et al., 2018)
Rab45	EF-hand pair	Unknown	(Wang et al., 2018)
TRAK1	CC1-box domain	Mitochondria	(van Spronsen et al., 2013)
TRAK2	CC1-box domain	Mitochondria	(van Spronsen et al., 2013)
HAP1	CC1-box domain	Many membrane cargos	(Caviston et al., 2007)
NUMA	CH domain	Minus-ends of MT in the spindle	(Hueschen et al., 2017)
CCDC88A	CH domain	Unknown	(Redwine et al., 2017)
CCDC88B	CH domain	Lysosomes	(Ham et al., 2015)
CCDC88C	CH domain	Unknown	(Redwine et al., 2017)
Hook2	Hook domain	Centrosomal proteins	(Szebenyi et al., 2007)
BICDL2	CC1-box domain	Rab13 vesicles	(M. A. Schlager et al., 2014)
BICD1	CC1-box domain	COP1-independent Golgi-ER vesicles	(Matanis et al., 2002)
JIP3*	RH1 domain	Activated JNK and lysosomes	(Arimoto et al., 2011)
RILP*	RH1 domain	RAB7 late endosomes, lysosomes	(Cantalupo et al., 2001)

Table S2 - Oligonucleotide sequences for sgRNAs, repair templates and PCR screening.

SGRNA'S	**OLIGONUCLEOTIDE SEQUENCES**
dli-1 Δ369-443 #1	fw cttgCTGGCAACTTCAACCACTA
	rv aaacTAGTGGTTGAAGTTGCCAG
dli-1 Δ369-443 #2	fw cttgGTTATGCATCACTGTCCCG
	rv aaacCGGGACAGTGATGCATAAC
dli-1 FF/AA #1	fw cttgTGGAGAAGAAATTGGCGAG
	rv aaacCTCGCCAATTTCTTCTCCA
dli-1 FF/AA #2	fv cttgAGCAAGTTGGAGAAGAAAT
	rv aaacATTTCTTCTCCAACTTGCT
dli-1 LL/AA #1	fv cttgTTTACCTTATTGAGCAAGT
	rv aaacACTTGCTCAATAAGGTAAA
dli-1 LL/AA #2	fv cttgTTCTCCAACTTGCTCAATA
	rv aaacTATTGAGCAAGTTGGAGAA

REPAIR TEMPLATES	**OLIGONUCLEOTIDE SEQUENCES**
dli-1 Δ369-443	AAGATCAGGCTTTCTTGAAGAAGTTGATGGACATCCTGGCA ACTTCAACCTAAGACAGTGATGCATAACGTCATTTTCATAAT CTATTTAAATATTTTAAGCT
dli-1 FF/AA	CCAAGCCGAGGACTATGCAAGAAGAGCCTACCGATAAGGA CAGTCCACTCGCCAATGCGGCGTCCAACTTGCTCAATAAGG TAAATCAATCTTAGATCTTTTTTCTATGTGA
dli-1 LL/AA	AAGAAGAGCCTACCGATAAGGACAGTCCACTCGCCAATTTC TTCTCCAACGCGGCCAATAAGGTAAATCAATCTTAGATCTTT TTTCTATGTGAATTTCCATATTTC

	OLIGONUCLEOTIDES FOR SCREENING
dli-1 Δ369-443	fw CCAGTGCAGCTCAAGTGATTG
	rv CCAAGTGATCTCTGTCCCCG
dli-1 FF/AA	fw CGATAAGCTTAGACCTGTCGCA
	rv CTTGCTCGGCTTGTCCTGA
dli-1 LL/AA	fw CAAGCCGAGGACTATGCAAGAA
	rv CAGACTTCAGAAGACGATCGAG